

## Cartography of the Luna-21 landing site and Lunokhod-2 traverse area based on Lunar Reconnaissance Orbiter Camera images and surface archive TV-panoramas



I.P. Karachevtseva<sup>a,\*</sup>, N.A. Kozlova<sup>a</sup>, A.A. Kokhanov<sup>a</sup>, A.E. Zubarev<sup>a</sup>, I.E. Nadezhdina<sup>a</sup>, V.D. Patratiy<sup>a</sup>, A.A. Konopikhin<sup>a</sup>, A.T. Basilevsky<sup>a,b</sup>, A.M. Abdrakhimov<sup>b</sup>, J. Oberst<sup>a,c,d</sup>, I. Haase<sup>d</sup>, B.L. Jolliff<sup>e</sup>, J.B. Plescia<sup>f</sup>, M.S. Robinson<sup>g</sup>

<sup>a</sup> Moscow State University of Geodesy and Cartography (MIIGAiK), MIIGAiK Extraterrestrial Laboratory (MExLab), Gorokhovskiy per., 4, 105064 Moscow, Russia

<sup>b</sup> Vernadsky Institute of Geochemistry and Analytical Chemistry, Russian Academy of Sciences, 119991, 19 Kosygin street, Moscow, Russia

<sup>c</sup> German Aerospace Center (DLR), 12489, 2 Rutherfordstraße, Berlin, Germany

<sup>d</sup> Technical University Berlin, 10623, 135 Str. des 17. Juni, Berlin, Germany

<sup>e</sup> Department of Earth and Planetary Sciences and the McDonnell Center for the Space Sciences, Washington University in St. Louis, Campus Box 1169, One Brookings Drive, St. Louis, MO 63130, USA

<sup>f</sup> The Johns Hopkins University, Applied Physics Laboratory, 20723, 11100 Johns Hopkins Road, Laurel, Maryland, USA

<sup>g</sup> School of Earth and Space Exploration, Arizona State University, 85281, Tempe, AZ, USA

### ARTICLE INFO

#### Article history:

Received 31 July 2015

Revised 24 March 2016

Accepted 10 May 2016

Available online 24 May 2016

#### Keyword:

Moon

Moon surface

Image processing

### ABSTRACT

The Lunar Reconnaissance Orbiter Camera (LROC) system consists of a Wide Angle Camera (WAC) and Narrow Angle Camera (NAC). NAC images (~0.5 to 1.7 m/pixel) reveal details of the Luna-21 landing site and Lunokhod-2 traverse area. We derived a Digital Elevation Model (DEM) and an orthomosaic for the study region using photogrammetric stereo processing techniques with NAC images. The DEM and mosaic allowed us to analyze the topography and morphology of the landing site area and to map the Lunokhod-2 rover route. The total range of topographic elevation along the traverse was found to be less than 144 m; and the rover encountered slopes of up to 20°. With the orthomosaic tied to the lunar reference frame, we derived coordinates of the Lunokhod-2 landing module and overnight stop points. We identified the exact rover route by following its tracks and determined its total length as 39.16 km, more than was estimated during the mission (37 km), which until recently was a distance record for planetary robotic rovers held for more than 40 years.

© 2016 Elsevier Inc. All rights reserved.

### 1. Introduction

Luna-21 landed on 16 January 1973 and deployed the roving vehicle Lunokhod-2 (Researches of the Moon, 1975). The goals of the mission were to study the topography, geology, and morphology of the lunar surface, in particular, the transition between mare and highlands. Luna-21 touched down in Le Monnier crater, located on the eastern margin of the Serenitatis Basin; the lava that filled Mare Serenitatis also flooded the floor of this 61 km diameter crater (Fig. 1).

After an initial reconnaissance of the surrounding area (Fig. 2a), the Lunokhod-2 vehicle (Fig. 2b) descended to the lunar surface and started its journey and scientific experiments. Soon

after landing the first panoramas and navigation images were taken and transmitted to Earth showing the surroundings, including the landing module (Fig. 3). Rover instruments, as well as equipment mounted on the first Soviet rover, Lunokhod-1 (Vinogradov, 1971; Barsukov, 1978), were to determine the physical and mechanical properties (Leonovich et al., 1971) and chemical composition of the lunar regolith (Viktorov and Chesnokov, 1978). Lunokhod-2, similar to Lunokhod-1, carried an X-ray telescope (Beigman et al., 1978), radiation detector (Vernov et al., 1971), and laser reflector for geodetic ranging experiments (Kokurin et al., 1978). As with Lunokhod-1, Lunokhod-2 was remotely controlled from the ground station in Crimea (Simferopol), but had a high degree of autonomy to enable it to operate for extended periods of time in the extreme conditions on the lunar surface (Kemurdzhian, 1993).

Lunokhod-2 survived for five lunar days and explored an area of approximately 180 km<sup>2</sup> (estimated using a rectangle surrounding

\* Corresponding author. Tel.: +7 4992673513.

E-mail address: [i\\_karachevtseva@miigaik.ru](mailto:i_karachevtseva@miigaik.ru) (I.P. Karachevtseva).

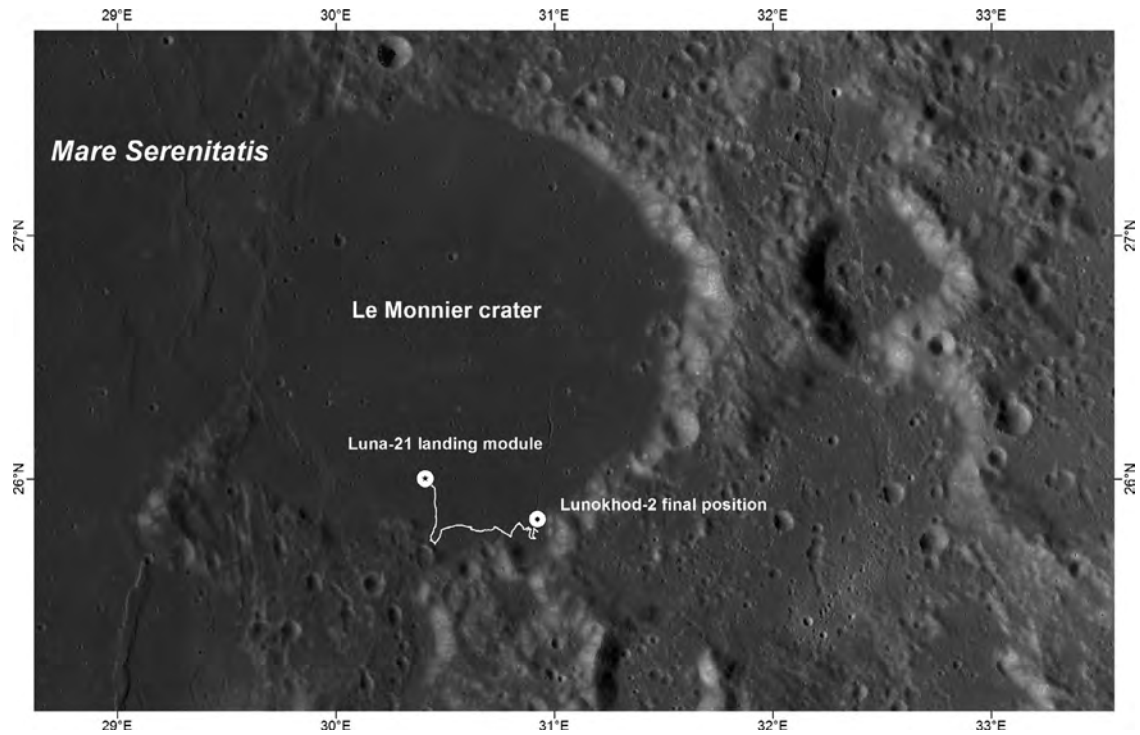


Fig. 1. Map of crater Le Monnier with Luna-21 landing area. Background: WAC global mosaic (Scholten et al., 2012).

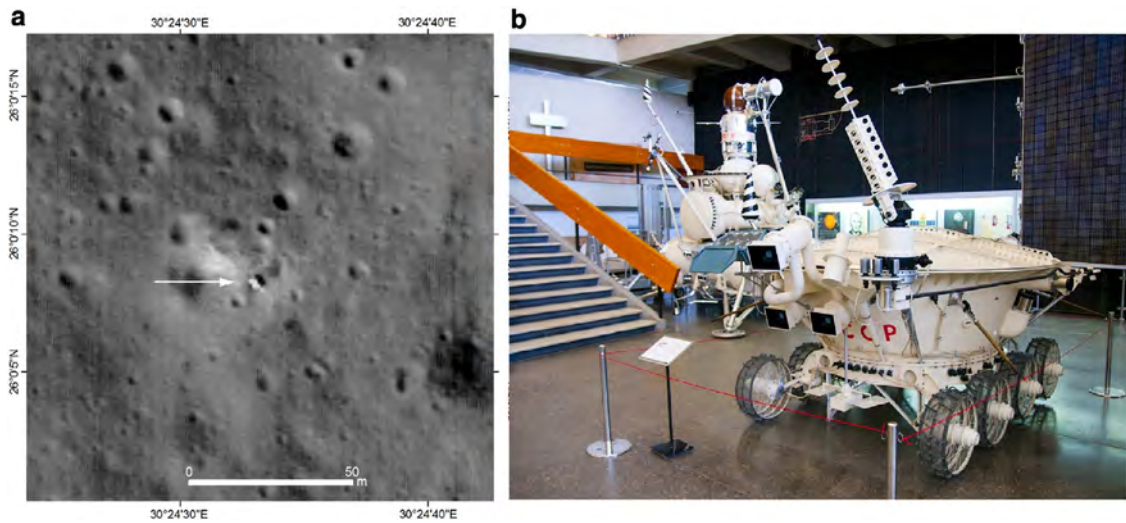


Fig. 2. (a) Landing area of the Luna-21 mission and landing module, LROC NAC M122007650L (NASA/GSFC/ASU)); and (b) a model of Lunokhod-2 in The State Museum of the History of Cosmonautics named by K.E. Tsiolkovskiy (Kaluga).

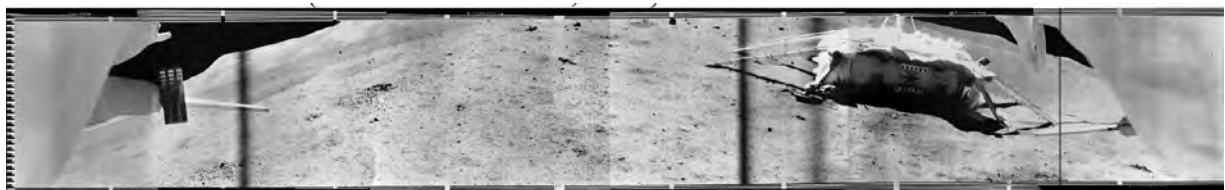


Fig. 3. Archive lunar panorama (#6-372) taken by Lunokhod-2 cameras on the first lunar day: the image, showing the Luna-21 landing module, is looking to the south; massifs of Le Monnier crater (left) are visible on the horizon ~10 to 15 km to the east.

the entire route). Onboard camera systems (Selivanov et al., 1971) provided more than 90 panoramas (Fig. 3) and 80,000 navigation images.

On April 20, Lunokhod-2 drove into a relatively small but steep-sloped crater. During an attempt to exit the crater the solar panel accidentally contacted the crater wall and scooped up and deposited soil onto the spacecraft radiator. On May 10, the temperature inside the spacecraft became critical and operation was stopped. Radio contact with the rover was lost a day later (May 11), due to overheating of the vehicle body (Dovgan, 2015). The mission was officially terminated 3 June 1973 (Huntress and Marov, 2011).

High-resolution images obtained by the Lunar Reconnaissance Orbiter Camera (LROC) Narrow Angle Camera (NAC) (Robinson et al., 2010) have renewed interest in this historic rover mission. The Luna-21 lander and the rover can clearly be identified in the NAC images and rover wheel tracks along the traverse can be studied (Table 1). Recently, interest in the accomplishments of Lunokhod-2 was renewed when the length of the traverse of the Mars rover Opportunity exceeded the Lunokhod-2 record of 39.22 km in April 2014, a record that was held for more than 40 years by Lunokhod-2.

In this paper, we report mission details and the Lunokhod-2 traverse measurements based on the NAC images and associated ephemeris.

## 2. Lunokhod-2

### 2.1. The rover construction and equipment

Construction of Lunokhod-2 (Fig. 2b) was similar to that of Lunokhod-1, and consisted of the same self-propelled chassis and the sealed instrument compartment containing the scientific equipment. The total mass of Lunokhod-2 was 836 kg compared to 756 kg of Lunokhod-1 (Kemurdzhian, 1993). The top of the instrument compartment was equipped with a thermal radiator that could be covered by a large retractable lid during the night to reduce heat loss (Elenov et al., 1971). The bottom side of the lid was equipped with solar arrays to supply power during the day. The solar cells were augmented with a combination of batteries and a polonium heat generator. New gallium arsenide solar arrays were deployed (instead of the previous siliceous photoelectric cells (<http://www.laspace.ru/rus/luna21.html>), providing a total capacity of 250 Ah (Lunokhod-1 had 200 Ah).

In addition to the scientific equipment available on the Lunokhod-1, Lunokhod-2 had notable improvements (Kemurdzhian, 1993), as follows:

- a third navigation camera that allowed the operator crew to better focus on lunar surface (Dovgan, 2015);
- a spectrometer RIFMA-M (Roentgen Isotopic Fluorescent Method of Analysis) that was used to determine the chemical composition of the lunar regolith (Kocharov and Viktorov, 1974) and had been modified in comparison to RIFMA on board Lunokhod-1 (Kocharov et al., 1971);
- a ternary ferromagnetometer, mounted on a remote arm (1.5 m length), that was to measure the magnetization of individual targets on the lunar surface (Dolginov et al., 1976);
- an astrophotometer for measuring the luminosity of the sky at visible and ultraviolet wavelengths (Severny et al., 1975).

Lunokhod-2 had eight wheels, four on each side of the rover body. Each wheel consisted of three titanium rings (510 mm in diameter) and 16 spokes wrapped in a metallic mesh. The wheels were 200 mm wide, and the spacing between wheels (track gauge) was 1600–1700 mm (Anisov et al., 1971). On soft surfaces the wheels were observed to penetrate deep into the regolith, and the

wheels formed pronounced tracks along its traverse. The average specific pressure of the wheels on the ground (at a nominal depth in the regolith of 30 mm) was 0.05 kg/cm<sup>2</sup> (Leonovich et al., 1978). The Lunokhod tracks are easily observed in the NAC frames because the grousers on the wheels significantly disturbed the soil. This disturbance is in marked contrast to the wheels of the Apollo lunar rover vehicles that did not have grousers and whose tracks are difficult to observe outside of the descent stage blast zones (Clegg et al., 2014), despite the fact that the wheel loading was similar.

Lunokhod-2 moved at two distinct speeds: 0.8 km/h and 2.0 km/h (Kemurdzhian, 1993). Turning of the vehicle was achieved by varying the rotation of the wheel on the right and left sides, respectively, and by changing the direction of their rotation. The turning radius of the rover in motion was typically 3 m with wheels turning at different speeds (Kemurdzhian, 1993). However, the rover could also turn in place (with its left and right wheels turning in opposite directions) within a radius of 0.8 m. Areas where the rover turned in place are detectable in the NAC images (see below Fig. 15a) and on archive images obtained by Lunokhod cameras (e.g. in Fig. 16a left).

The rear of the instrument compartment contained the heat source (polonium 210), the lifting and lowering mechanism for the lid (Kemurdzhian, 1993), as well as an experiment with a penetrator, PROP (Russian abbreviation from PRibor Otsenki Prokhodimosti, an instrument to measure trafficability) for assessments of physical and mechanical properties of the regolith (Cherkasov and Shvarev, 1975). Lunokhod-2 had an improved system of automatic locks that reacted in the event that the rover encountered dangerous slippage on steep slopes or excess voltage in the onboard power system.

Lunokhod-2 was equipped with a laser reflector, consisting of a block of 14 prisms (45 × 20 × 8 cm<sup>3</sup>) made of special heat-resisting glass and protected by multi-layer heat-insulating material (Kokurin et al., 1978). Since 1978 regular laser measurements of Lunokhod-2 carried out at the Crimean Astrophysical Observatory (CrAO) using a 2.6-m telescope provided data on the distance to the Moon with an accuracy of 25 cm (Kokurin, 2003). Results from the Lunar Laser Ranging (LLR) experiment provided important insights concerning the dynamics and interior of the Moon (Dickey et al., 1994). In addition, with the reflector coordinates established to the cm level, the laser reflector stations mark important geodetic reference points that define the currently used lunar coordinate systems (Archinal et al., 2011). At CrAO, a total of 1400 measurements were made using the Lunokhod-2 laser reflector; these observations were terminated in 1983 owing to cancellation of the Soviet lunar program (Kokurin, 2003). However, the Lunokhod-2 laser ranging was continued from other observatories (Williams et al., 2013), unlike the case of its predecessor on Lunokhod-1, which could not be recovered until its recognition in LRO images (Murphy et al., 2011). For unknown reasons, the return signal from Lunokhod-2 is at least five times weaker than that of Lunokhod-1. One possible explanation is that lunar dust is obscuring the reflectors (Murphy et al., 2010).

### 2.2. Lunokhod-2 navigation system

The number of Lunokhod cameras and their locations were chosen to give full view of the surrounding area, including horizon, the Sun, the Earth, as well as to provide information about the ground surface for safe movement.

Lunokhod-1 had two television cameras for navigation (abbreviated as “MKTV” - the Russian abbreviation stands for “small frame television system”) mounted at a height of 950 mm above the surface, the average height of a seated person (Selivanov et al., 1971). At the request of the operator crew (Dovgan, 2015),

**Table 1**  
Images used for DEM processing and mosaicking.

Number of images	Image IDs	Date and time	Pixel scale, m	Emission angle, deg	Solar azimuth, deg	Incidence angle, deg
1.	M101971016LE	11.07.2009, 17:02	1.5	14.58	183.64	82.99
2.	M101971016RE	11.07.2009, 17:02	1.5	17.35	183.22	83.23
3.	M106669064LE	04.09.2009, 02:04	1.67	17.64	228.29	37.54
4.	M106669064RE	04.09.2009, 02:04	1.67	14.87	226.38	37.75
5.	M106683404RE	04.09.2009, 06:02	1.5	1.21	219.92	38.79
6.	M109039075LE	01.10.2009, 12:23	0.56	15.00	82.67	27.42
7.	M109039075RE	01.10.2009, 12:23	0.56	12.23	83.06	27.41
8.	M119646179LE	01.02.2010, 06:48	0.56	3.74	196.34	59.43
9.	M119646179RE	01.02.2010, 06:48	0.56	0.92	195.52	59.50
10.	M122007650LE	28.02.2010, 14:46	0.56	11.40	220.83	36.53
11.	M122007650RE	28.02.2010, 14:46	0.56	8.64	219.53	36.59
12.	M129086218LE	21.05.2010, 13:02	0.56	1.64	162.36	56.23
13.	M129086218RE	21.05.2010, 13:02	0.56	1.13	162.51	56.30
14.	M131440712LE	17.06.2010, 19:04	0.56	18.78	176.39	80.26
15.	M131440712RE	17.06.2010, 19:04	0.56	21.60	176.11	80.34
16.	M139707174LE	21.09.2010, 11:18	0.56	4.57	249.57	28.40
17.	M139707174RE	21.09.2010, 11:18	0.56	7.50	248.53	28.42
18.	M146783727LE	12.12.2010, 09:01	0.9	1.68	172.21	75.46
19.	M146783727RE	12.12.2010, 09:01	0.92	1.13	172.20	75.52
20.	M165645602LE	18.07.2011, 16:25	0.5	0.68	190.95	70.12
21.	M165645602RE	18.07.2011, 16:25	0.56	1.13	190.27	70.18
22.	M168000478LE	14.08.2011, 22:33	0.5	27.13	218.90	47.61
23.	M168000478RE	14.08.2011, 22:33	0.5	24.36	216.81	47.65
24.	M172717196LE	08.10.2011, 12:45	0.57	0.89	116.66	30.03
25.	M172717196RE	08.10.2011, 12:45	0.57	3.66	117.02	30.05
26.	M175070494LE	04.11.2011, 18:27	0.57	25.73	154.18	47.90
27.	M175070494RE	04.11.2011, 18:27	0.57	28.50	153.82	47.94
28.	M177426582RE	02.12.2011, 00:55	0.57	23.63	171.04	71.52
29.	M177433351LE	02.12.2011, 02:48	0.57	17.53	280.48	70.67
30.	M177433351RE	02.12.2011, 02:48	0.57	14.76	166.34	70.73
31.	M180966502LE	12.01.2012, 00:13	1.52	1.78	190.57	70.57
32.	M183325364RE	08.02.2012, 07:28	1.51	1.20	206.51	46.39
33.	M185684246LE	06.03.2012, 14:42	1.4	1.78	243.23	27.22
34.	M188035994LE	02.04.2012, 19:58	1.49	6.19	125.17	28.92
35.	M188035994RE	02.04.2012, 19:58	1.49	9.17	125.58	29.04
36.	M188043142LE	02.04.2012, 21:57	1.49	1.78	122.85	28.65
37.	M1105709502LE <sup>a</sup>	24.10.2012, 09:17	1.36	16.27	150.69	45.29
38.	M1105709502RE <sup>a</sup>	24.10.2012, 09:17	1.36	19.04	150.63	45.49
39.	M1105723789RE <sup>a</sup>	24.10.2012, 13:15	1.36	4.44	146.08	43.95
40.	M1105723789LE <sup>a</sup>	24.10.2012, 13:15	1.36	7.21	145.43	43.78
41.	M1108074725RE	20.11.2012, 18:17	1.48	1.20	166.77	67.48
42.	M1108074725LE	20.11.2012, 18:17	1.48	1.77	166.60	67.27
43.	M1113965174RE <sup>a</sup>	27.01.2013, 22:32	1.37	6.51	205.18	48.81
44.	M1113965174LE <sup>a</sup>	27.01.2013, 22:32	1.37	9.27	206.37	48.62
45.	M1113986482RE <sup>a</sup>	28.01.2013, 04:27	1.37	29.72	200.53	51.28
46.	M1113986482LE <sup>a</sup>	28.01.2013, 04:27	1.37	26.95	200.94	51.03
47.	M1118681776RE	23.03.2013, 12:42	1.26	1.13	117.53	27.11
48.	M1118681776LE	23.03.2013, 12:42	1.26	1.64	116.90	27.02
49.	M1123399010LE	17.05.2013, 03:03	1.4	1.64	170.50	68.45
50.	M1126921794RE <sup>b</sup>	26.06.2013, 21:36	1.39	3.84	187.12	75.25
51.	M1126921794LE <sup>b</sup>	26.06.2013, 21:36	1.39	6.61	187.78	75.04
52.	M1126928906LE <sup>b</sup>	26.06.2013, 23:34	1.39	1.36	186.92	75.57
53.	M1126928906RE <sup>b</sup>	26.06.2013, 23:34	1.39	4.13	186.36	75.77
54.	M1126936017LE <sup>b</sup>	27.06.2013, 01:32	1.30	9.79	186.37	76.08
55.	M1126936017RE <sup>b</sup>	27.06.2013, 01:32	1.30	12.74	185.87	76.29
56.	M1129282798LE	24.07.2013, 05:26	1.39	1.64	202.72	52.45
57.	M1129282798RE	24.07.2013, 05:26	1.39	1.13	201.77	52.64
58.	M1131636702LE	20.08.2013, 11:17	1.28	1.64	230.85	33.17
59.	M1131636702RE <sup>a</sup>	20.08.2013, 11:17	1.28	1.13	229.59	33.30

<sup>a</sup> Images used for DEM production (Table 2).

<sup>b</sup> Images used for mosaicking (Fig. 10).

Lunokhod-2 was equipped with a third MKTV-camera mounted above the others, that would provide a view of the traverse ahead from the height of a standing person. This camera was a significant improvement and proved very useful when elements of the rover's attitude control system failed after landing. The driver and the crew had to navigate the rover based on the positions of the Sun and prominent relief features (Dovgan, 2015). The average speed of Lunokhod-2 was 340 m/h (in contrast to the average speed of Lunokhod-1 of 140 m/h). The high speed of Lunokhod-2

was obtained because operators benefitted from the experience of Lunokhod-1 (Petrov, 1978; Dovgan, 2015), as well as more frequent (closely spaced) navigation frames (approximately every 6 s vs. every 20 s for Lunokhod-1), which was enabled by a higher data transmission rate (Kemurdzhian, 1993).

In order to conduct the topographic and morphologic study of the lunar surface, the rover was also equipped with four panoramic scanner cameras: one horizontal and one vertical on each side (Selivanov et al., 1971). The cameras had a scanning

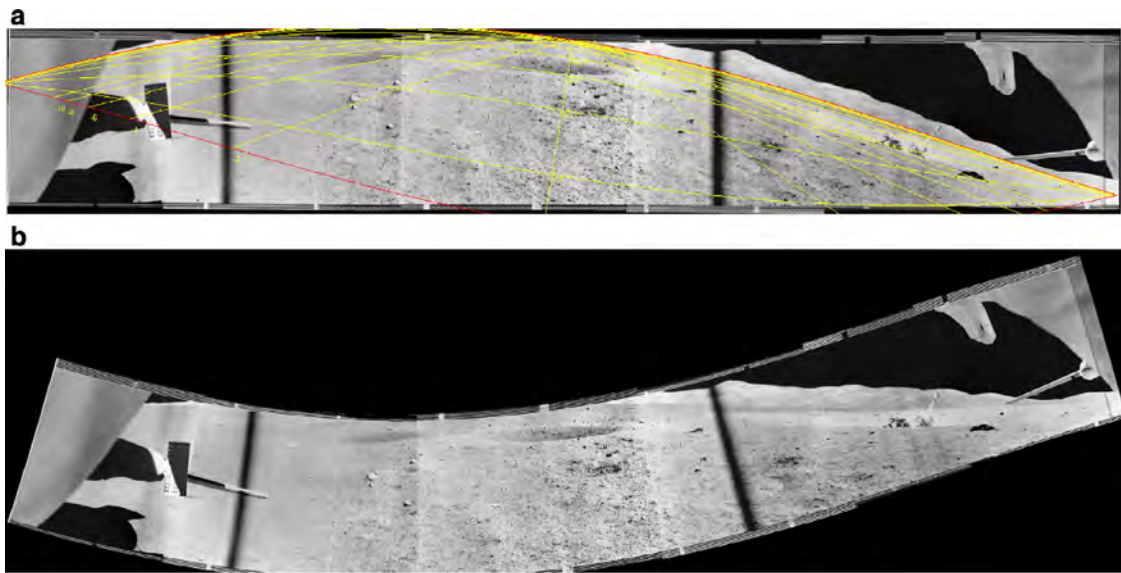


**Fig. 4.** The first Lunokhod-2 panorama taken from the lunar surface looking to the east (#6-368). A small crater and the landing module (right) resting on the flat mare plain are seen in the foreground while the highland mountains composing the rim of Le Monnier crater can be seen in the background: (a) image with superimposed coordinate grid for tilt measurements; and (b) the same image corrected for horizon curvature.

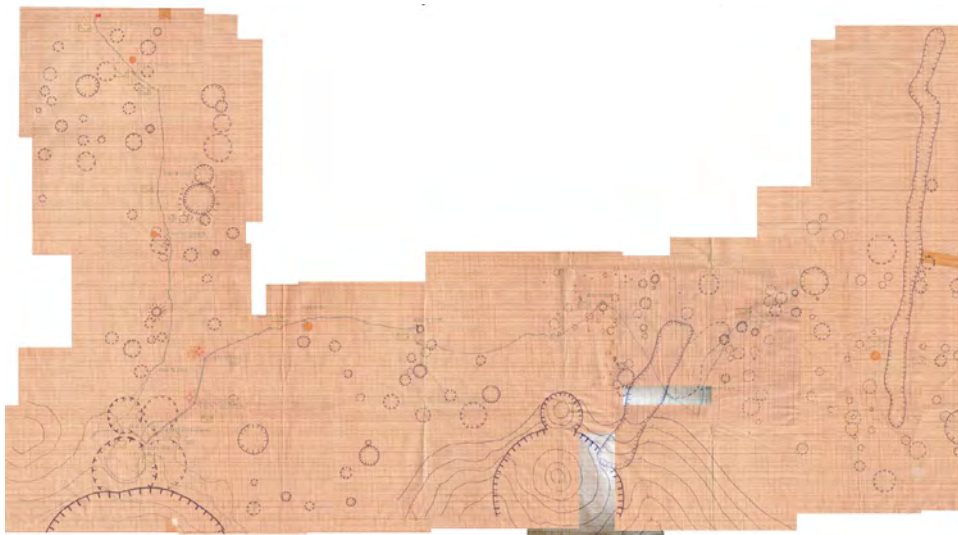


**Fig. 5.** Historic operations map of the Lunokhod-2 traverse, compiled during the mission (Lavochkin Research and Production Association Museum).

mirror which made rotational and oscillatory motion to form a panoramic image of about 3000 lines ( $180^\circ$ ) per 500 samples ( $30^\circ$ ) for horizontal view (Figs. 3 and 4a) and 6000 lines ( $360^\circ$ ) per 500 samples ( $30^\circ$ ) – for vertical view. Stereo images at some selected sites were obtained by taking panoramas from two positions of the Lunokhod (Rodionov et al., 1971). Based on stereo panoramas some topographic maps were obtained, which allowed to determine the steepness and slopes inside craters (Fig. 6b). For photogrammetric processing and elevation measurements exterior orientation parameters were derived from views to the Sun, the Earth and to distant surface objects like the rim of Le Monnier crater (Rodionov et al., 1973).

Unfortunately, details on the orientation parameters including coordinates and tilts of the rover are not available and must be considered lost. To recover coordinates we implemented a method (Kozlova et al., 2014) that is based on a search for panorama observation points on LROC NAC images. The Lunokhod tilts have to be determined iteratively using archive panoramic images. Specially developed software (Zubarev et al., 2016), including digital

palette (Fig. 4a), provides reconstruction of the horizon line with different values of tilts. After adjusting to the visible skyline on the panorama, the image is corrected for horizon geometric distortion (Fig. 4b).

### 2.3. Previous reconstruction of the route

The original operations map of the Lunokhod-2 route (Fig. 5) based on traverse measurements during the mission, is currently held by the Lavochkin Research and Production Association Museum (<http://www.laspacespace.ru/rus/museum.php>). This map was compiled using photogrammetry and geodesy techniques that were initiated in the MIIGAiK Aerial Survey Department by Boris Nepoklonov in 1966. Later in the frame of navigation tasks of the Lunokhod-1 mission (Rodionov et al., 1971), the methodology was improved in the Space Research Institute of the Russian Academy of Science (Rodionov, 1999).

Using a combination of individual topographic maps of small study areas derived from operative panorama processing based on coordinate observations and navigation measurements, various maps of the Lunokhod-2 route were produced by the Nepoklonov group (Rodionov et al., 1973), including a topographic map of the southwest part of the route (Fig. 6a), a relief map of an intensively studied small crater (Fig. 6b), and a topographic sketch map of the entire working area (Fig. 7); the last of these maps was published later (Kemurdzhian et al., 1978). The maps show craters and depressions, central hills of craters, individual boulders, and areas with scattered small rocks along the route (Lipskiy and Rodionova, 1978). The landing site, locations where samples were taken for the chemical analyses of the regolith, selected points for panoramic and stereoscopic surveys, rover stop points of RIFMA, and magnetic experiments have been marked. For our new analysis these maps provided important information (see Tables 6 and 7).

The first geologic map (Fig. 8a) based on results of a geomorphologic study of the Lunokhod-2 area (Florensky et al., 1974), as well as the geomorphologic sketch map (Fig. 8b) derived from analyses of Le Monnier crater (Florensky et al., 1976; see also recent geologic review in Abdrakhimov, 2009) were compiled on the basis of the Lunokhod-2 route map.

More recently, the Lunokhod-2 study area was investigated using Clementine UV-VIS images with 100-m resolutions (Stooke, 2007) and NAC images (Abdrakhimov et al., 2011).

### 3. LRO data image processing

#### 3.1. LRO mission

The Lunar Reconnaissance Orbiter (LRO) was launched on June 18, 2009. After commissioning, LRO moved in a nearly circular, 50 km, polar orbit during its first year of operation (Vondrak et al., 2010). For a period of one month this orbit was changed to a slightly elliptical orbit for low-periapsis passes and higher-resolution imaging, from approximately 21 km above the mean surface. With its extended science mission beginning in December 2011, LRO transferred to an elliptical (40 × 200 km<sup>2</sup>) energy-saving “frozen orbit” (see Keller et al., 2016).

#### 3.2. Camera and images

The LROC WAC obtains images at moderate resolution (100 and 400 m pixel scale) at ultraviolet and visible (321–689 nm) seven-color, whereas the two identical NACs provide high-resolution (0.5 m/pixel from 50 km altitude) monochrome images (Robinson et al., 2010). The NAC images are 5000 pixels wide and typically 52,224 lines long. Using adjacent orbits and with spacecraft tilt, the NAC acquires overlapping stereo pairs ideally suited to produce high-resolution DEMs, and geometrically accurate orthoimages (Oberst et al., 2010; Scholten et al., 2012).

The Lunokhod-2 area as well as other lunar landing sites, such as Apollo 17 (Haase et al., 2011) and Luna-17 (Karachevtseva et al., 2013) are LROC priority targets, the Luna-21 area has been imaged many times with varying pixel scales, viewing, and illumination conditions (Table 1).

#### 3.3. Stereo image processing

For the DEM and orthoimage production based on photogrammetric techniques, we used 59 NAC images (<http://wms.lroc.asu.edu/lroc>) of the study area (Table 1). Pre-processing was conducted by means of specially developed software (Zubarev et al., 2016) using preliminary exterior orientation parameters (coordinate position of LROC NAC cameras) (Mazarico et al., 2012), provided by Spacecraft Position Kernels (SPKs) and temperature cor-

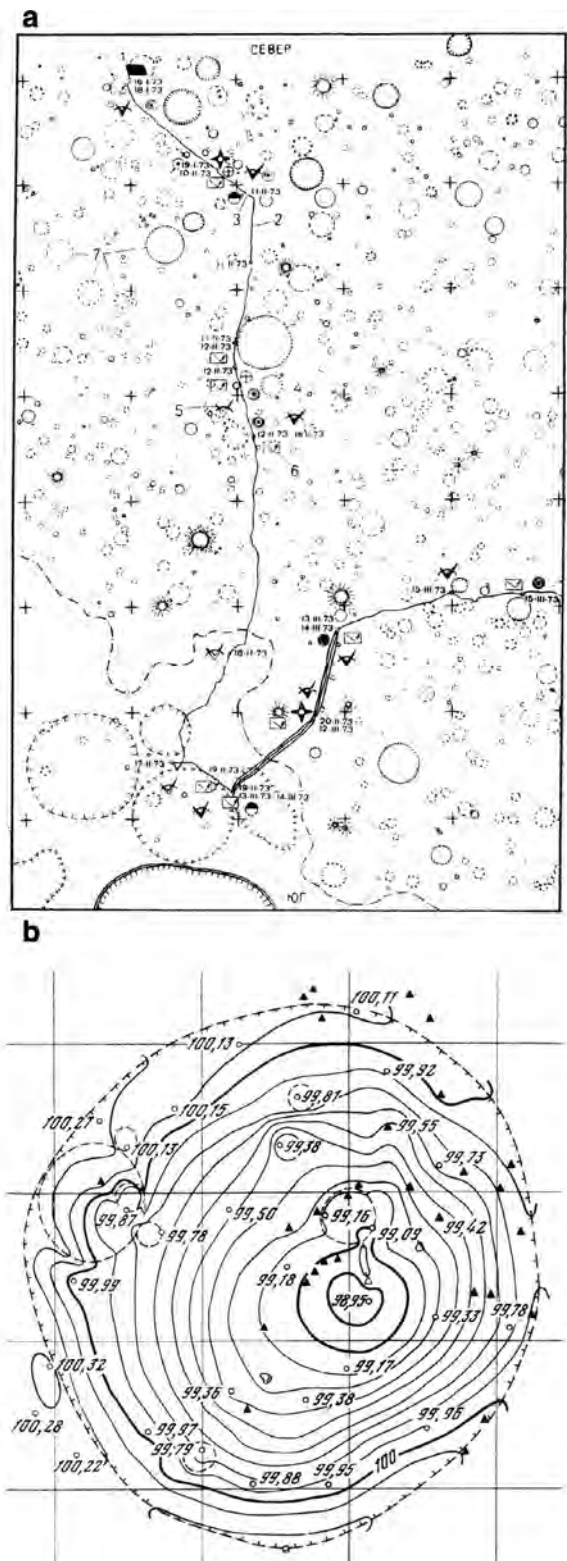


Fig. 6. Detailed maps of the Lunokhod-2 study area (Rodionov et al., 1973): (a) topographic map on southwest part with “triple traverse”, where the rover moved three times along the same traverse (original scale 1: 50,000); and (b) relief map of one of the small craters (original scale 1: 100); diameter  $D = 9.5$  m;  $H = 1.4$  m.

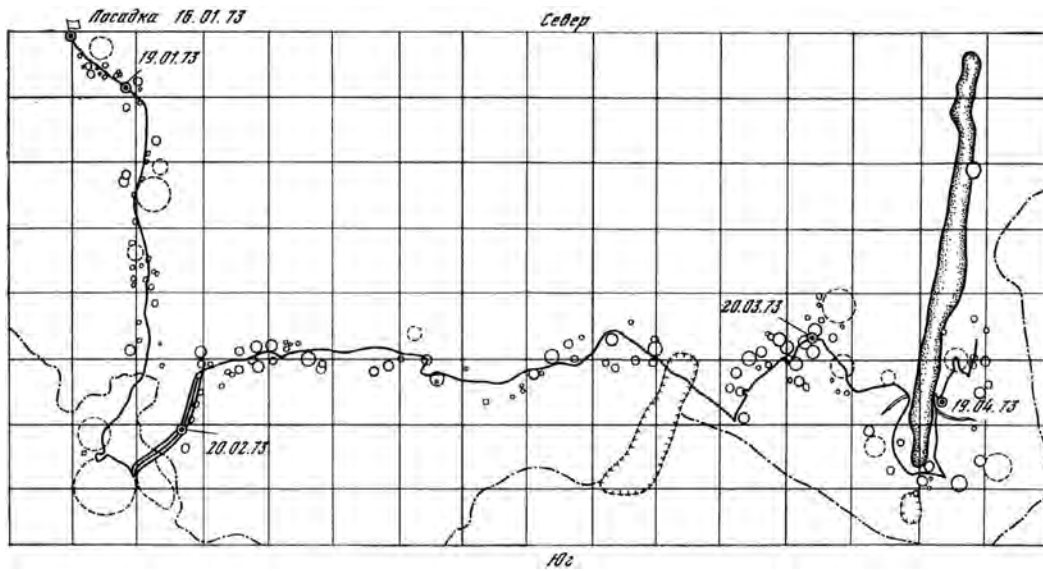


Fig. 7. A topographic sketch map of Lunokhod-2 route (Kemurdzhian et al., 1978).

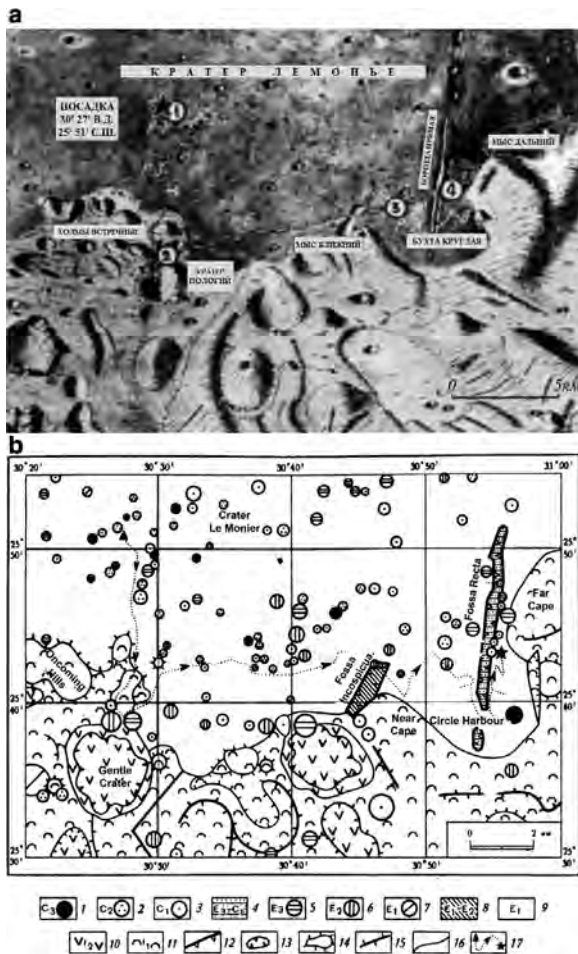


Fig. 8. (a) Historic geologic map of Lunokhod-2 region, compiled by G.A. Burba. When first published (Florensky et al., 1974), unofficial names were used for lunar objects in the study area (here in Russian; for English names see panel b). (b) Geomorphologic sketch map of Lunokhod-2 exploration area (Florensky et al., 1976): 1–3 – Late, Middle and Early Copernican craters; 4 – Fossa Recta; 5–7 – Late, Middle and Early Eratosthenian craters; 8 – Fossa Inconspicua; 9 – Le Monnier lava-flooded crater floor; 10 – Late Imbrian craters; 11 – Le Monnier crater rim; 12 – tectonic scarps; 13 – large crater rims; 14 – hill slopes; 15 – ridges; 16 – geomorphologic boundaries; and 17 – Lunokhod 2 route.

rected C-matrix Kernels (Speyerer et al., 2012) taken from SPICE (<http://naif.jpl.nasa.gov/naif/data.html>) at the selected time. Using this same software all images were converted from PDS-format (\*.img) to an internal format of the digital photogrammetry system PHOTOMOD (Adrov et al., 1995).

In the next step, 342 tie-points, covering all images (Table 1), were measured based on semi-automatized correlation method in PHOTOMOD version 5.3 (<http://www.racurs.ru/?page=634>). The average number of measurements for each tie-point, using various images, is 10 and the maximum is 18. A least-squares bundle block adjustment was carried out, resulting in improved position and orientation parameters of the NAC images. The PHOTOMOD implementation of the block adjustment is based on the RPC model (Grodecki and Dial, 2003), which is characterized by an effectively reduced number of adjustment parameters (6 per image) providing a numerically stable solution. Considering the average pixel size of 1.0 m, the coordinate accuracy on the lunar surface (RMS errors) were estimated as  $RMS_x = \pm 1.8$  m,  $RMS_y = \pm 3.9$  m,  $RMS_z = \pm 4.3$  m.

The NAC typically obtains nadir images (consequently, emission angles are close to  $1^\circ$ , see Table 1), however, the spacecraft was occasionally tilted to obtain stereo images for targets of interest (resulting in emission angles of  $>10^\circ$ ) with convergence more than  $5^\circ$ . As images were obtained at different times of the day, illumination varies accordingly, so only 5 stereo pairs obtained under similar lighting conditions, as recommended for automated 3-D terrain processing (Becker et al., 2015), were chosen for creating the DEM covering the entire Luna-21 activity area; for each of the 5 pairs the difference in solar azimuth and solar incidence angle amounts to less than  $15^\circ$ , suitable for image correlation in a single pair.

We produced the DEM with a resolution of 2.5 m/pixel (Fig. 9) based on algorithms of automatic relief generation using a semi-global approach (Hirschmüller, 2005), which uses the iterative-deformation method implemented in PHOTOMOD software (Sechin, 2014). This method takes into account the result of transformation (deformation) of multiple overlapping elevation models produced in several iterations. In the first iteration a preliminary elevation model  $H_0$  (level 0) is used, interpolated from the measured tie-points. In the next steps transformations are made with various elevation models  $H_{\pm i}$  looking for maximal coefficient of correlation between overlapping models during  $i$ -iterations at one level.

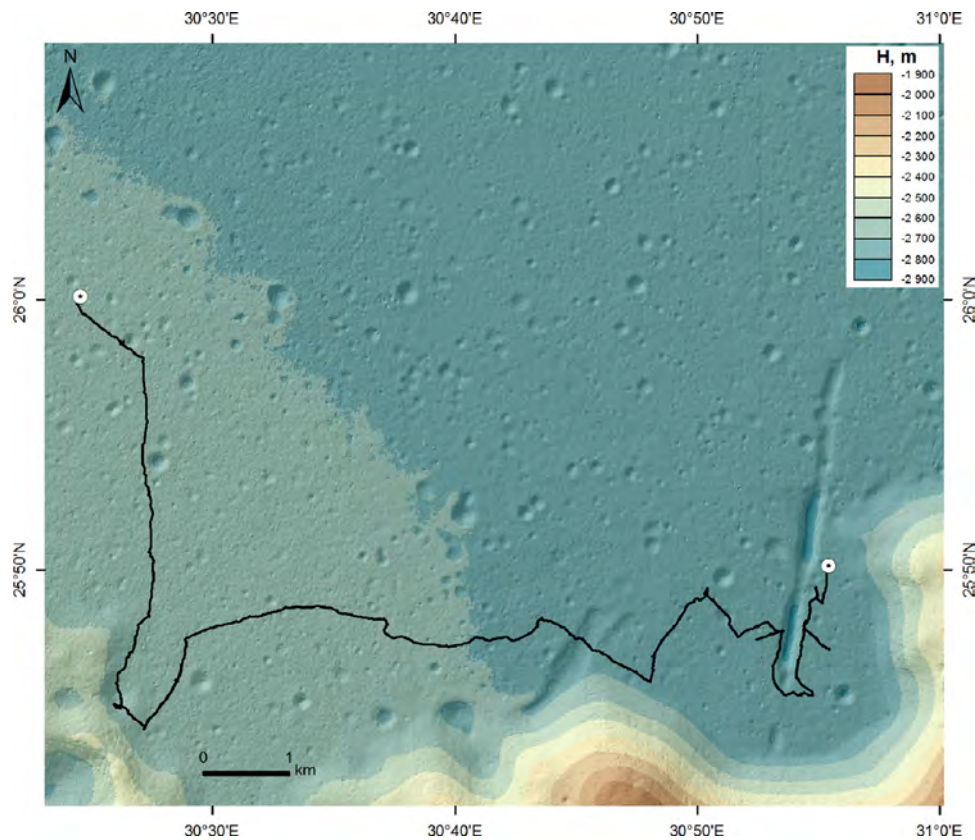


**Fig. 9.** DEM of the Lunokhod-2 area with the resolution of 2.5 m/pixel produced from photogrammetric processing of NAC images using PHOTOMOD software (background – hillshade relief derived from DEM).

Finally, data with favorable conditions (Table 1) – both with high resolution and similar illumination (with small discrepancy in solar azimuth and incidence angle from images taken from sequential orbits; in our case time difference not more than 4 h) – were selected for mosaicking (Fig. 10) for further analysis and mapping.

The results of the photogrammetric image processing (DEM and orthomosaic) provide a consistent coordinate system for the Lunokhod-2 area derived from an absolute accuracy of orientation parameters of the NAC cameras in the lunar coordinate system. Using the processed stereo pair M1113986482RE and M1113965174RE, the coordinates of the final position of Lunokhod-2 in stereo mode have been determined (Table 3). The derived coordinates are related to the ground surface point under the rover (not to the lid of Lunokhod-2). The nominal (a priori) accuracy of elevation determination for the selected stereo pair is 1.7 m.

Comparing of the Lunokhod-2 final position coordinates obtained in this study from stereo measurements (Table 3) with LLR derived positions (Williams et al., 2013) shows an average discrepancy of ~118 m. To remove this (absolute) positional error, the DEM and the orthomosaic were controlled to the LLR derived coordinates of the final position of Lunokhod-2 by shifting them in latitude and longitude (assuming rotational offsets to be minimal). Using the transformed data as a basis for the spatial measurements, all coordinates of this paper are given in the LLR system (see Tables 6 and 7). The remaining errors of the coordinates are as follows: elevation accuracy is  $\pm 3$  m derived from maximal value of nominal elevation accuracy of the DEM (2.9 m, Table 2); RMS error of plane coordinates is  $\pm 2$  m derived from nominal resolution of images used for orthomosaicking (1.4 m, Table 1) and operator error (1 pixel).

**Table 2**

Parameters of LROC NAC stereo pairs used for DEM production.

Number of pairs	Image IDs	Angle of convergence, deg	Nominal elevation accuracy, m
1	M1131636702RE–M1113986482RE	32.2	1.8
2	M1113986482RE–M1113965174RE <sup>a</sup>	38.6	1.7
3	M1105709502LE–M1105723789LE	25.5	2.9
4	M1105709502RE–M1105723789RE	25.2	2.9
5	M1113986482LE–M1113965174LE	39.3	1.8

<sup>a</sup> Stereo pair used for measurements of the Lunokhod-2 final position.

## 4. Study of Lunokhod-2 area

### 4.1. Traverse identification

The Lunokhod-2 route primarily extends from west to east (contrary to Lunokhod-1, which moved south to north), and Lunokhod-2 travelled a distance four times longer than Lunokhod-1. Hence, several sets of NAC images were required to cover the Lunokhod-2 study area. These images were acquired over several different LRO mission phases.

For track identification we used the highest-resolution NAC images, taken under complementary illumination conditions, as the visibility of the wheel tracks strongly depends on solar azimuth and incidence angle, similar to crater identification (Florensky et al., 1978; Basilevsky et al., 2012). In high Sun illumination, the tracks are very difficult to identify (Fig. 11a), whereas with low Sun (big solar incidence angle), the tracks are clearly visible (Fig. 11b). For the analysis of the traverse we used an orthomosaic (Fig. 11c) that includes images with best visibility of the track (81% of the

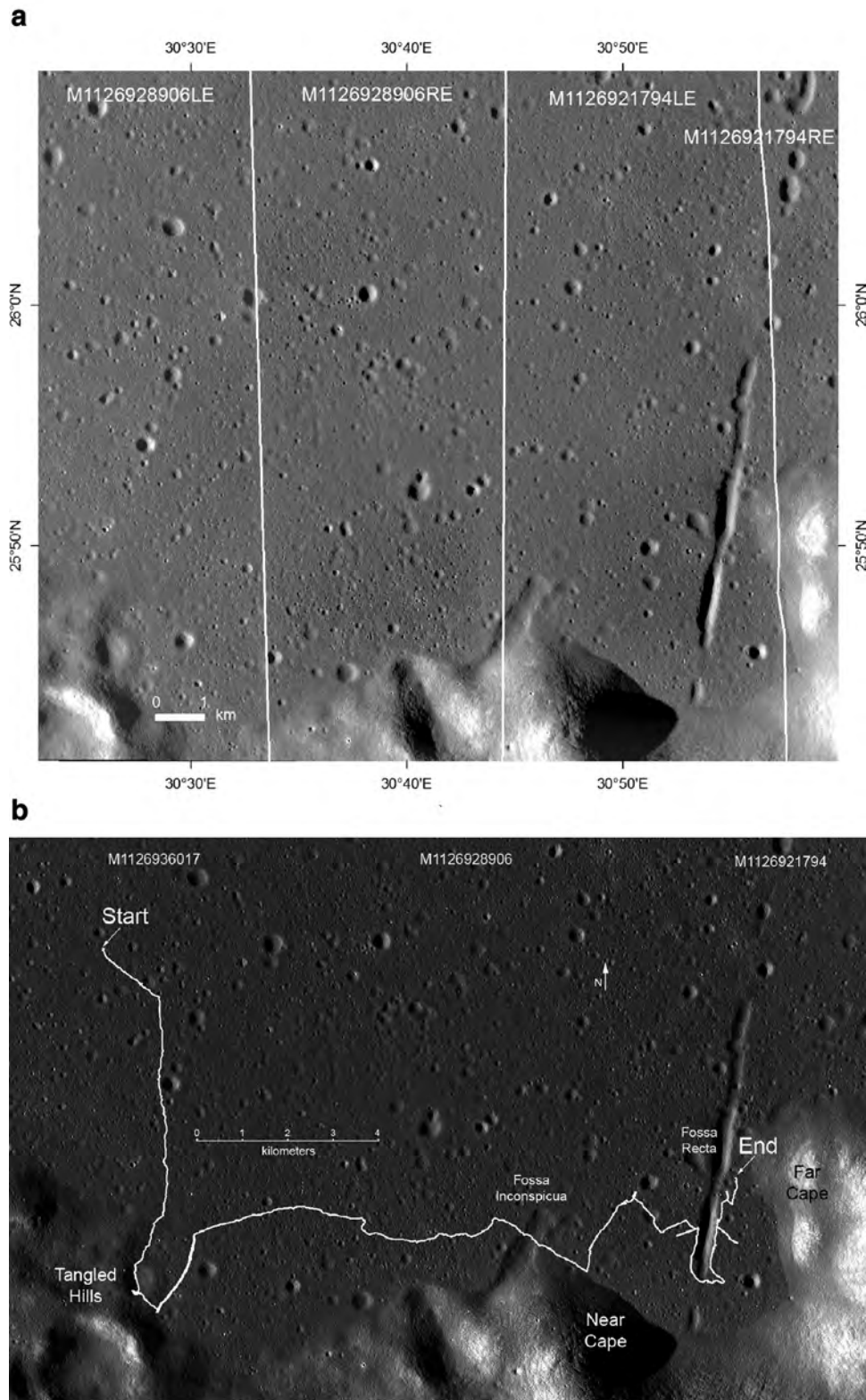


**Fig. 10.** (a) Orthomosaic of the Lunokhod-2 area with a resolution of 2.5 m/pixel produced from NAC images and DEM using PHOTOMOD software; and (b) NAC image mosaic with annotation showing the traverse route as traced on individual images.

**Table 3**

Comparison of stereo measurements (this study) and Lunar Laser Ranging (Williams et al., 2013) for final position of Lunokhod-2.

	X, m	Y, m	Z, m	Longitude, deg	Latitude, deg	Elevation, m
Lunokhod-2 coordinates (LLR)	1339388.601	802309.554	755849.750	30.9221056	25.8323282	−2761.338
Lunokhod-2 coordinates (LROC NAC DEM)	1339294.5	802303.9	755918.3	30.92371	25.83558	−2807.1
Differences	94.1	5.6	−68.6	−0.00160	−0.00325	45.8

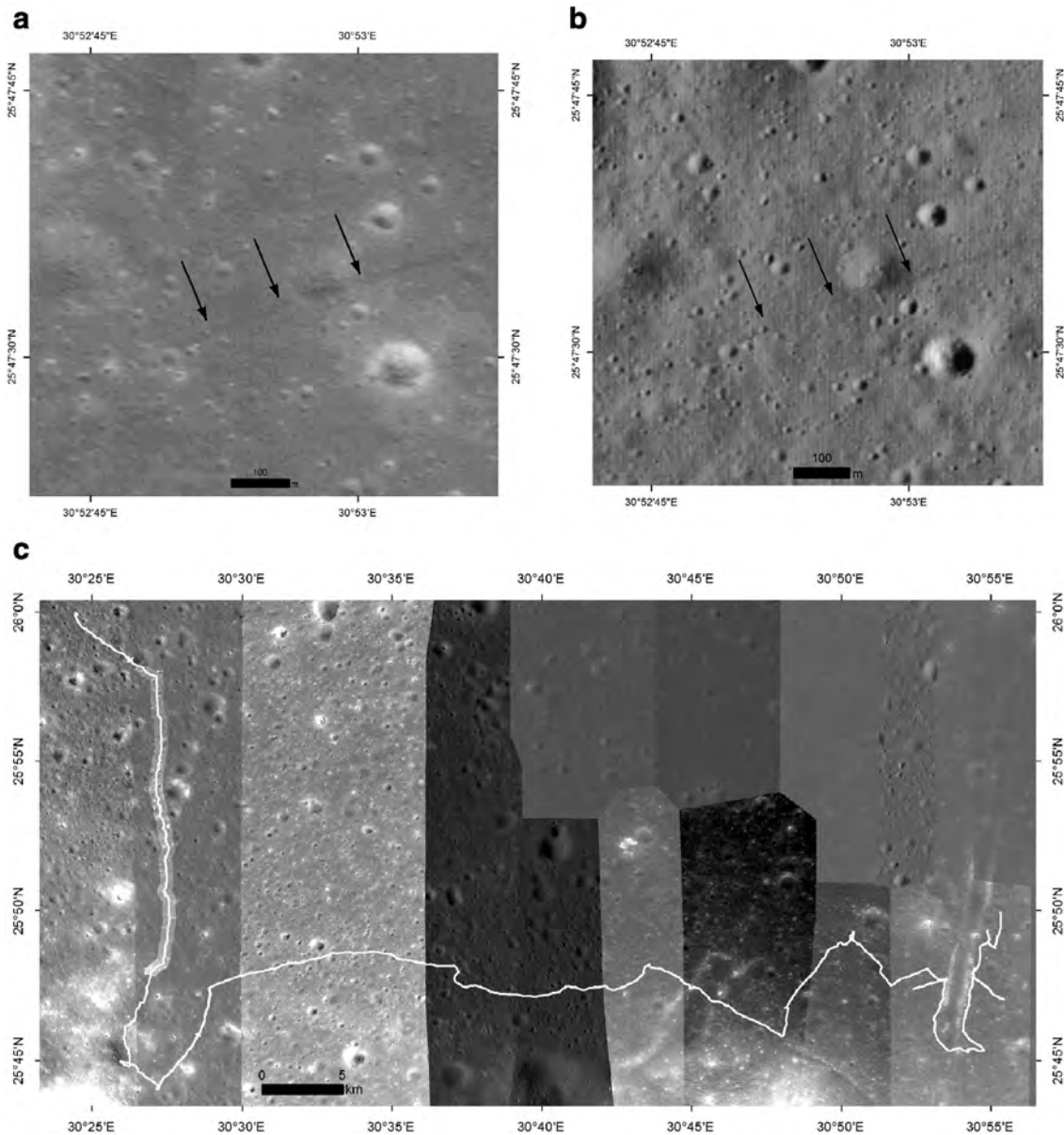


**Fig. 11.** Lunokhod-2 route on various LROC NAC images with different illumination conditions: (a) poor visibility of traverse with high Sun (image M109039075LE, solar incidence angle 27°); (b) good visibility of traverse with low Sun (image M177433351RE, solar incidence angle 71°); (c) orthomosaic with high quality visible track, produced to identify the route (equidistant cylindrical projection with center at study area – main meridian 30°40', standard parallel 25°50' – is used for all maps in the paper).

mosaic is covered by images with pixel scales of  $\sim 0.5$  m and 19%, about 1.0 m).

The Lunokhod-2 traverse was digitized using ArcGIS 10.3 (<http://www.esri.com/>) and in ISIS3 using the program Qview (Anderson et al., 2004). To obtain the most accurate positions for the traverse we used two different methods and software implementations: (1) 3D-stereo measurements in original stereo images, using PHOTOMOD, and (2) 3D-measurements in ArcGIS using the DEM.

After the identification of the traverse, the lengths of individual parts of the Lunokhod-2 traverse, from different lunar days, have been determined (Table 4). The total length of the traverse was measured to be 39.1 km (average from both techniques), significantly longer ( $\sim 2$  km) (Table 4) than the previously published result of 37 km, which was based on the onboard odometer measurements (<http://www.laspacespace.ru/rus/luna21.html>).

The discrepancy between historic and modern distance measurements (Fig. 12) probably has multiple causes: (1) lost navigation equipment after landing; (2) accumulated errors along path;

**Table 4**  
Lunokhod-2 route measurements.

Lunar day	Date	Description	New distances measured in GIS (this study), m	Distances measured by Lunokhod-2 9th wheels during Luna-21 mission (Dovgan, 2015), m
1	16.01–24.01.1973	Lunokhod-2 moved to the southeast	1299	1148
2	08.02–22.02.1973	Lunokhod-2 moved to the south. Study of crater with a diameter of 720 m. Turn to east	10,034	9919
3	09.03–21.03.1973	Lunokhod-2 moved east. Crossed the depression width 400 m, depth 27 m. Turned to the northeast	17,622	16,533
4	08.04–22.04.1973	Lunokhod-2 moved to the southeast - to southern tip of Fossa Recta. Traversed around Fossa Recta from the south to the north	9136	8600
5	08.05–10.05.1973	Lunokhod-2 moved to the north along Fossa Recta	1014	880
Total			$\Sigma$ 39,105	$\Sigma$ 37,080

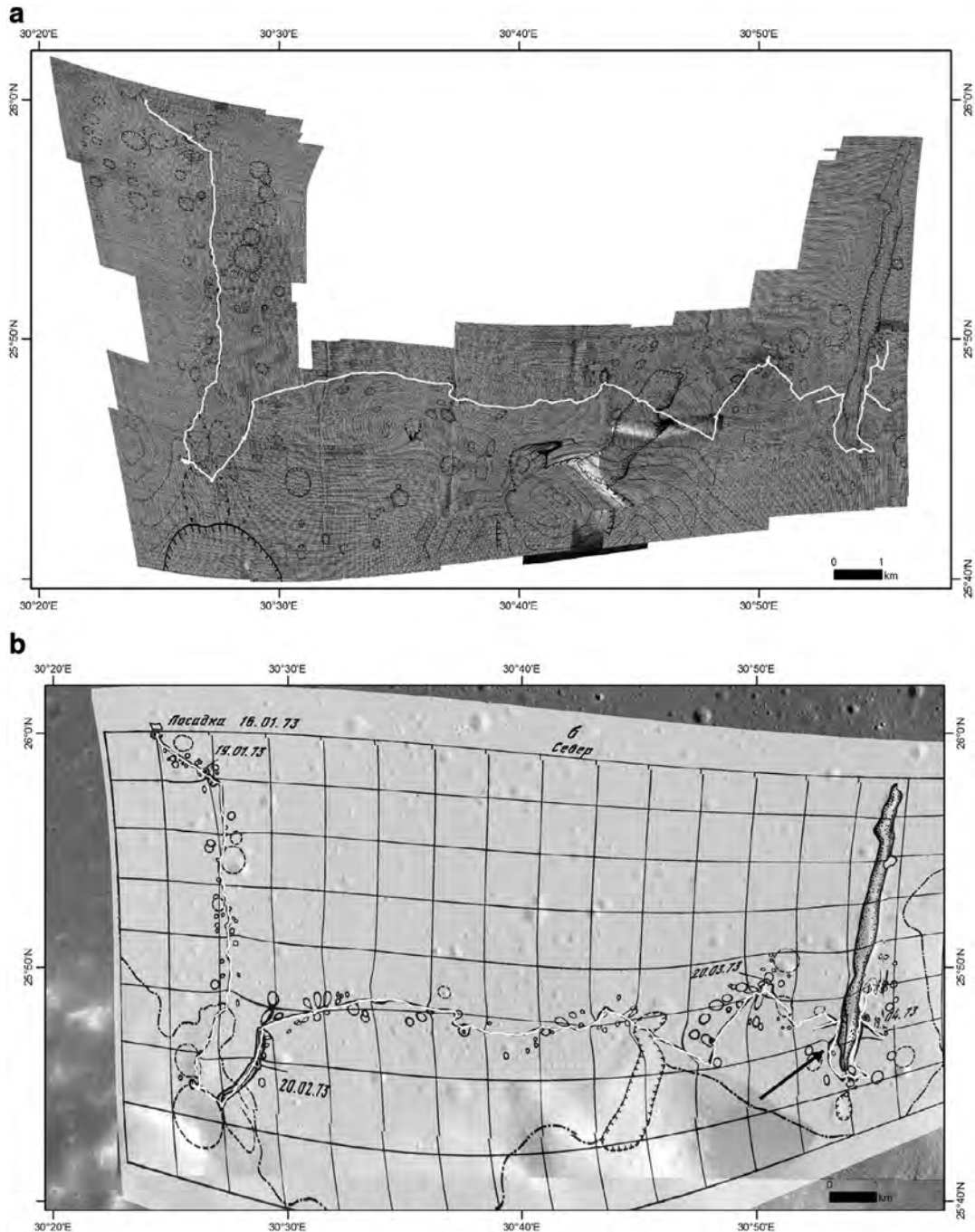


**Fig. 12.** Differences between Lunokhod-2 route, digitized in GIS (white), and the route from transformed historic map (black): (a) operative schema produced during Luna-21 mission; and (b) topographic schema, produced as result of analysis and mapping after mission (maximal discrepancy is about 80 m).

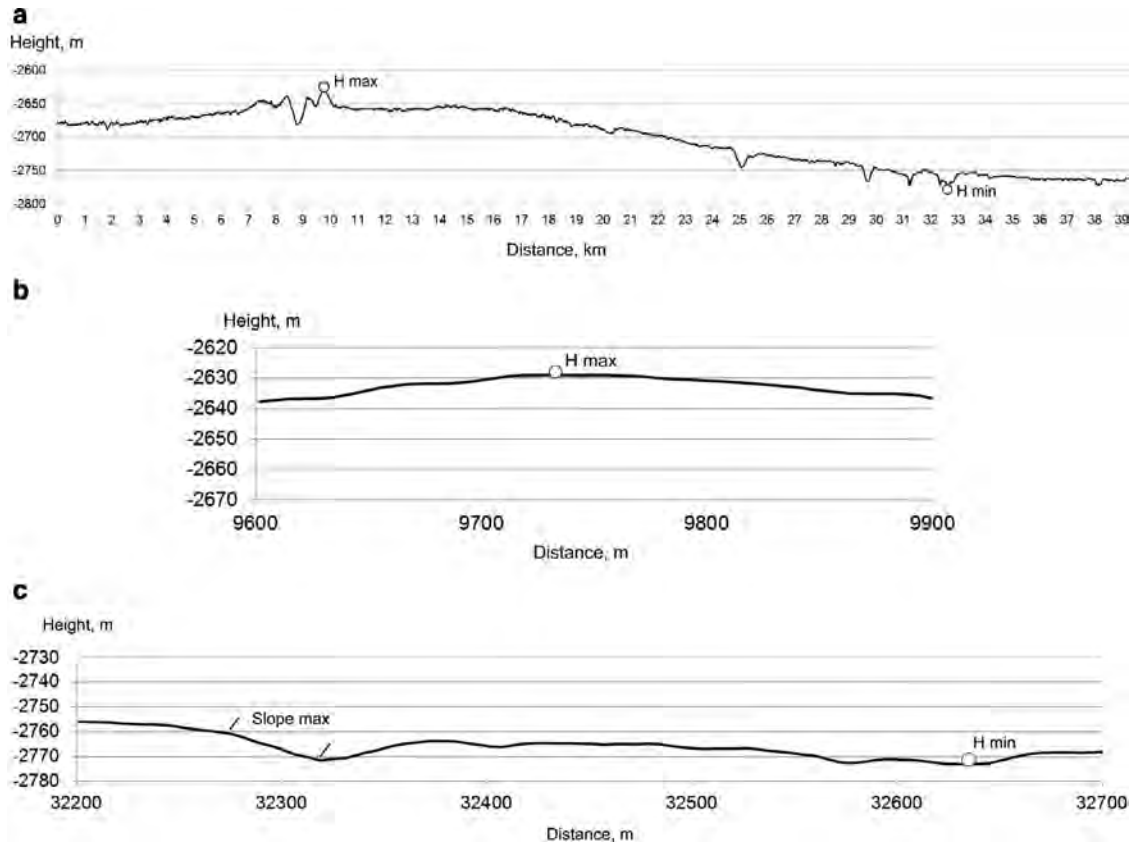


**Fig. 13.** Topographic profile of Lunokhod-2 route: (a) elevations along the route (vertical exaggeration = 20); (b) portion of route with maximum elevation; and (c) portion of route (near Fossa Recta) with lowest elevation and the maximum slope.

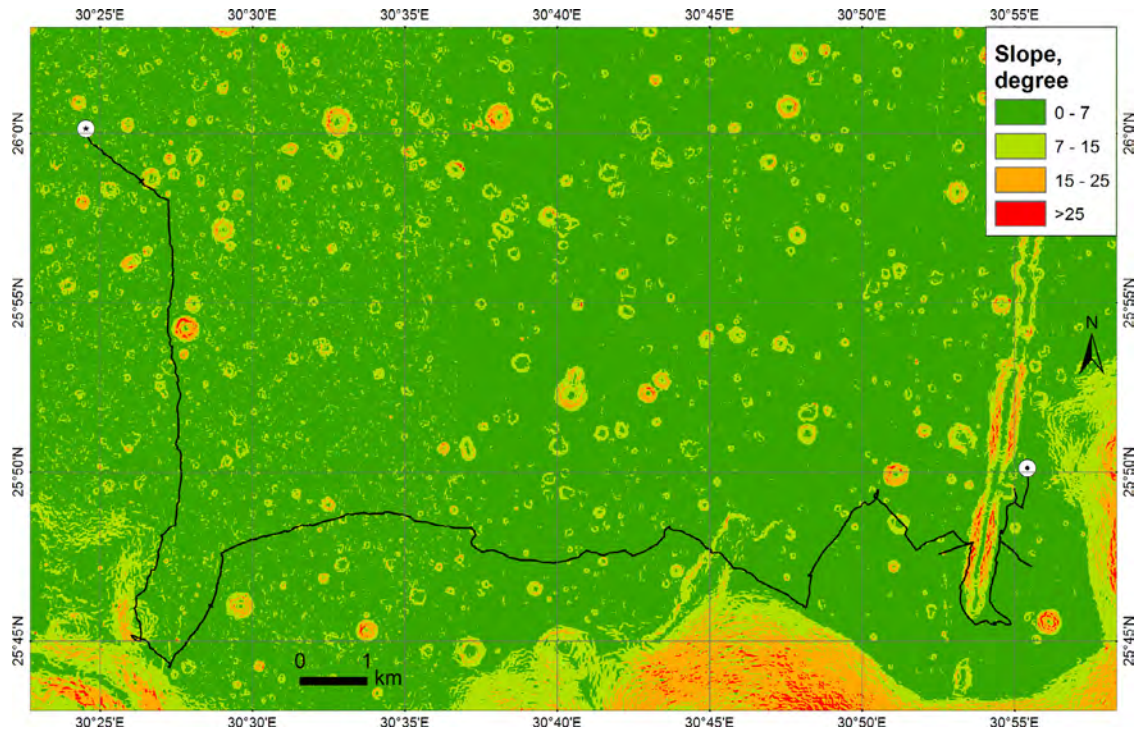


**Fig. 14.** Slope map for the Lunokhod-2 area computed using NAC DEM on a baseline of 5 m.

**Table 5**  
Slope analysis for the Lunokhod-2 area.

Slopes, deg	Area, km <sup>2</sup>	%
0–7	209.9	81.7
7–15	29.0	11.3
15–25	15.3	6.0
>25	2.6	1.0
Total	256.8	100

**Table 6**  
Lunokhod-2 overnight positions, measured in GIS.

Lunar night	Date	Longitude, deg	Latitude, deg	Elevation, m
1	25.01.1973–07.02.1973	30.43749	25.97351	–2678
2	23.02.1973–08.03.1973	30.47531	25.76436	–2657
3	22.03.1973–08.04.1973	30.84048	25.82145	–2736
4	22.04.1973–08.05.1973	30.91493	25.82212	–2769

(3) mistakes based on odometer measurements (9th wheel); and (4) differences between two methods of measurements (odometer and digitizing tracks). Despite the differences, two old maps manually referenced to tracks digitized in GIS show a good correlation between various data, demonstrating the excellent navigation work that was done during the Luna-21 mission (Fig. 12).

#### 4.2. Morphometric analysis

Based on the DEM and the digitized track, morphometric parameters of the Lunokhod-2 route were analyzed. We extracted a

**Table 7**  
Lunokhod-2 points of interest, measured in GIS.

No.	Lunar day	Date	Description	Longitude deg	Latitude, deg	Elevation, m
1.	1	16.01.1973	Landing site: First panoramic images taken from Luna-21 module (6-364–6-367) <sup>a</sup>	30.40754 <sup>b</sup>	25.99910 <sup>b</sup>	–2677
2.	1	16.01.1973–18.01.1973	The first panorama obtained from the lunar surface by Lunokhod-2: 6-368 (Fig. 4)	30.40705	25.99947	–2678
3.	1	16.01.1973–18.01.1973	Panoramic images near Luna-21 landing module: 6-370–6-374	30.40776	25.99926	–2678
4.	2	09.02.1973	RIFMA experiment and the first special magnetic experiment Panoramas 6-386–6-393	30.43749	25.97350	–2678
5.	2	11.02.1973–12.02.1973	RIFMA experiment	30.45223	25.90731	–2671
6.	2	12.02.1973	RIFMA experiment	30.45234	25.89795	–2670
7.	2	12.02.1973–16.02.1973	RIFMA experiment	30.45742	25.87743	–2670
8.	2	19.02.1973	Maximum elevation on the route RIFMA experiment	30.44376	25.74316	–2629
9.	3	12.03.1973	The second special magnetic experiment RIFMA experiment Panoramas 6-416–6-424	30.47489	25.76455	–2658
10.	2, 3	19.02.1973, 13.03.1973	South point of tripled traverse, crater with landslides RIFMA experiment Panoramas 6-410–6-415	30.45239	25.73441	–2653
11.	3	14.03.1973	North point of tripled traverse RIFMA experiment	30.48155	25.79006	–2658
12.	3	15.03.1973	RIFMA experiment	30.54591	25.80803	–2670
13.	3	16.03.1973	RIFMA experiment	30.61975	25.79995	–2694
14.	3	18.03.1973	RIFMA experiment	30.72665	25.80347	–2716
15.	3	21.03.1973	RIFMA experiment	30.84048	25.82145	–2736
16.	4	11.04.1973–15.04.1973	West side of Fossa Recta graben – start point of magnetic experiment RIFMA experiment Panoramas 6-444–6-447	30.89129	25.79523	–2764
17.	4	10.04.1973–15.04.1973	West side of Fossa Recta graben – end point of magnetic experiment	30.87385	25.78983	–2749
18.	4	15.04.1973–16.04.1973	Minimum elevation on the route	30.89013	25.78517	–2773
19.	4	16.04.1973–20.04.1973	East side of Fossa Recta graben – start point of magnetic experiment RIFMA experiment Panoramas 6-448–6-450	30.90668	25.79656	–2762
20.	4	16.04.1973–20.04.1973	East side of Fossa Recta graben – end point of magnetic experiment	30.92409	25.78380	–2763
21.	5	10.05.1973	Final position of Lunokhod-2	30.92211	25.83233	–2761

<sup>a</sup> ID of panoramic images based on Russian State Archive metadata.

<sup>b</sup> Comparison of Luna-21 landing site position with the coordinates obtained by (Wagner et al., 2014) based on mean values from images with improved SPKs (Speyerer et al., 2014) shows good results.

topographic profile (Fig. 13) and computed slopes along the traverse (Fig. 14).

The highest point of the traverse is –2629 m (Fig. 13b), located in the so-called Tangled Hills (or Encounter Hills), visited by the rover on the second lunar day of its journey. The lowest point (–2773 m) was encountered on the western side of Fossa Recta during the fourth lunar day (Fig. 13c). Here, the rover encountered maximum slopes at an angle of 20.3° measured on a baseline of 5 m. The total range of elevations along the Lunokhod-2 traverse is 144 m.

The slope analysis for the Lunokhod-2 area has been done using the DEM (Table 5). For spacecraft landing safety, a rather flat area was chosen for the Luna-21 module near the south rim of Le Monnier crater. Most slopes do not exceed 7° (about 82%); slopes of 7–15° are infrequent (~11%); areas with steep slopes (15 up to 25°) are rare (7%), and high slopes almost never occur (1%).

Using the crater catalog for a small portion of the Lunokhod-2 area near Fossa Recta and the high-resolution DEM, a detailed morphometric study and analysis of degradation of small impact craters on the lunar mare was made by Basilevsky et al. (2014). The analysis of cumulative frequency distributions of depth/diameter ( $d/D$ ) of the studied craters and derived crater degradation rate revealed two different processes of crater degradation: one is rather rapid and affects craters with  $d/D$  larger than ~0.14 and the maximum slope of crater inner wall steeper than ~25°; the other, significantly slower process, affects shallower craters with gentler slopes. Also, differences between obtained  $d/D$  of small impact craters with the earlier published values (Basilevsky, 1976) have been noted.

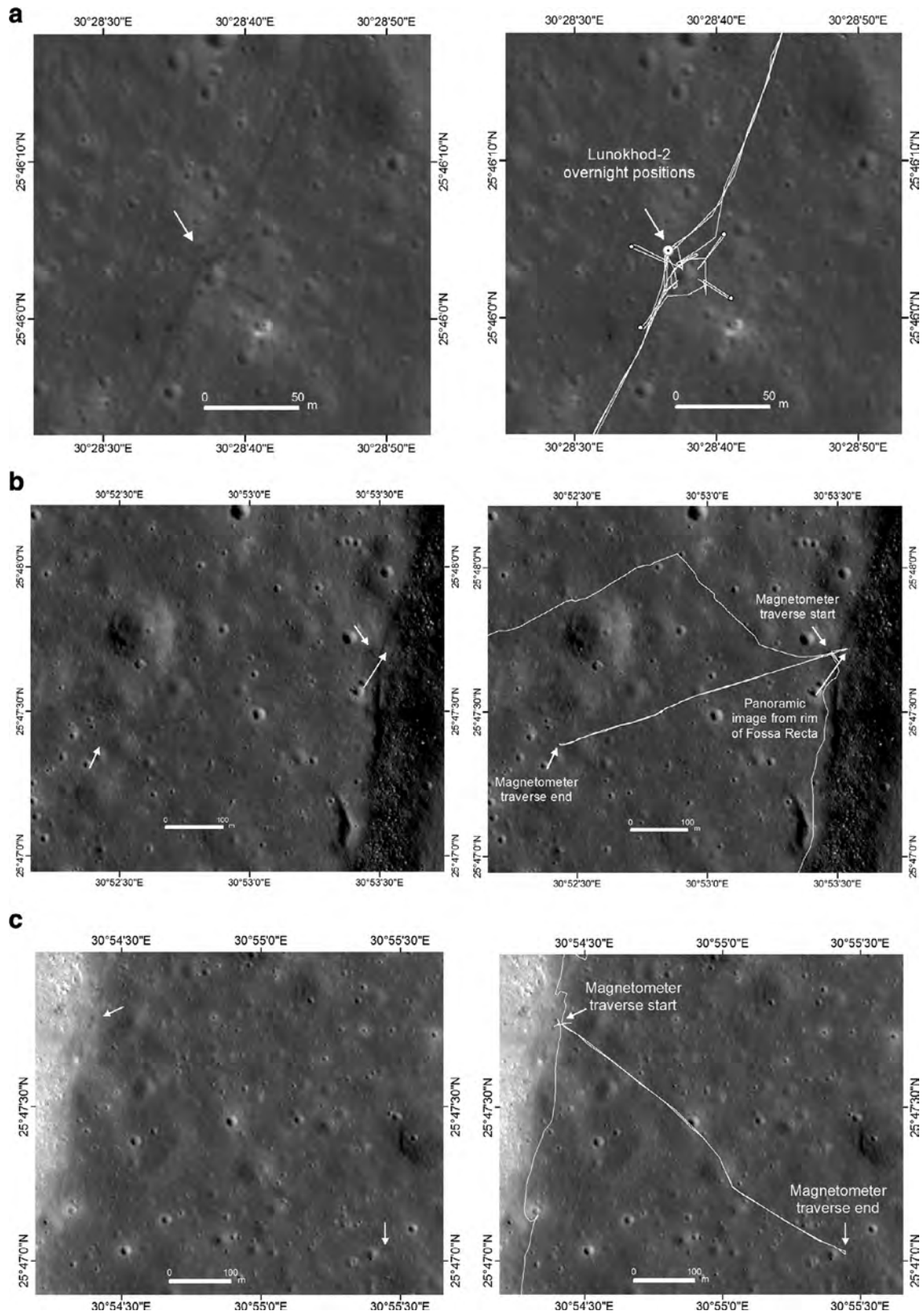


**Fig. 15.** Enlarged portions of the Lunokhod-2 route. The left images represent scenes from the original mosaic while the right show highlights of various stops and traverses from the Lunokhod-2 mission: (a) the southwest magnetometer traverse where the rover moved three times along this same traverse; (b) the west magnetometer traverse near Fossa graben; and (c) the east magnetometer traverse near Fossa graben.

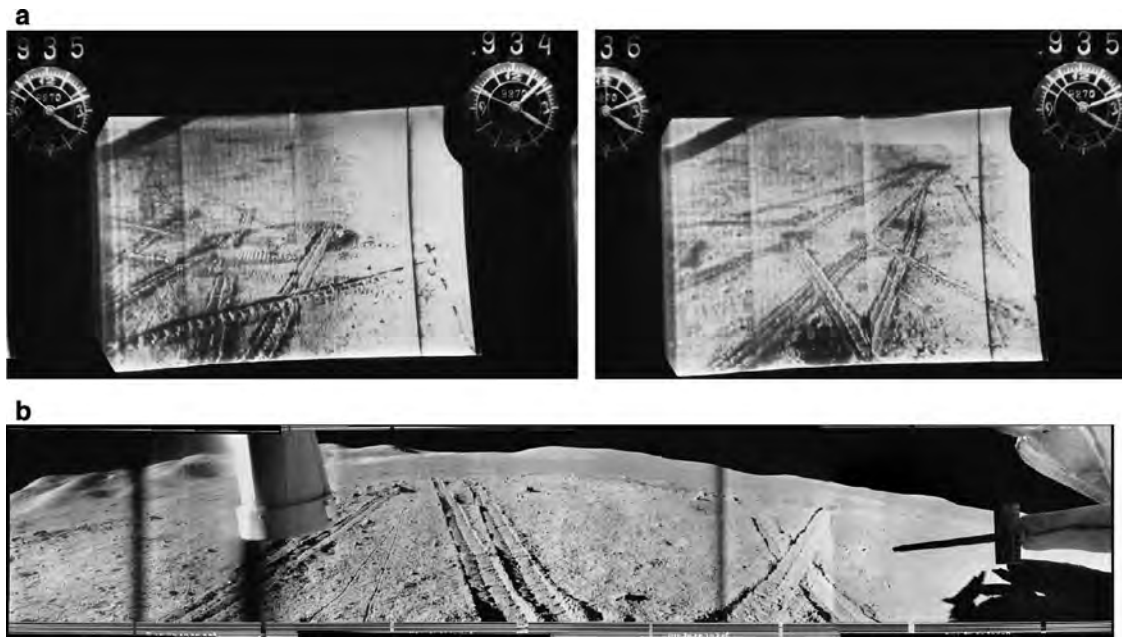


**Fig. 16.** Images taken by Lunokhod-2 navigation and panoramic cameras during the magnetic experiment on the third lunar day: (a) examples of MKTV-images; and (b) example of archive panorama (#6-387) shows tracks of the rover and its ninth wheel.

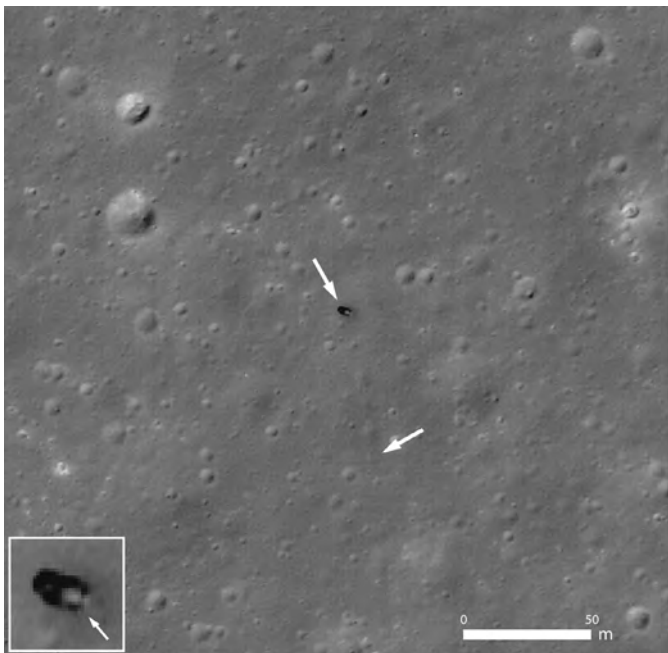


**Fig. 17.** Lunokhod-2 final position as seen in NAC image M175070494 (NASA/GSFC/ASU). The rover, the traverse, and the rover with open lid (zoomed inset) are marked by white arrows.

#### 4.3. Mission time line – Lunokhod-2

The automated spacecraft Luna-21 landed January 1, 1973 in the eastern part of the Sea of Serenity, in the southern portion of Le Monnier crater (30°24'E, 25°59'N), close to the edge of a 40 m crater. As for the landing of Luna-17, the engine of Luna-21 shut down only when the platform touched the lunar surface, not based on a signal from the gamma-altimeter “Quantum-2” as originally planned (Dovgan, 2015). After initial visual inspection of the site, the Lunokhod-2 rover descended to the lunar surface and began its journey, including scientific experiments and panorama

surveying (Tables 6 and 7). On the first lunar day, soon after landing, the first panoramas and navigation MKTV-images were taken and transmitted to the Earth showing the surroundings (Figs. 3 and 4).

Initially, Lunokhod-2 moved southwards and on the second lunar day (February 2, 1973) it reached the Tangled Hills (the closest part of the rim of Le Monnier crater). There, the Lunokhod-2 traveled uphill and studied the highlands. The main scientific goals of the mission were to study the transition zone between the mare and highlands and to examine prominent geologic features of the Fossa Recta (to the east from the landing site). Methods of study of the lunar surface were based on operational experience of Lunokhod-1 (Florensky et al., 1978). The approach combined detailed studies at selected points on the surface and studies along the traverse. The results of the detailed local studies can be considered as reference points and extrapolated along the corresponding part of the traverse. Comparison of quantitative characteristics obtained at such reference points shows changes in the surface properties along the traverse.

Several magnetic measurements were made during the mission (Dolginov et al., 1976). The magnetometer was mounted on a rod 1.5 m away from the rover; however, electrical currents inside the Lunokhod created magnetic fields that influenced the instrument readings. To eliminate this influence and perform the measurements, the rover moved away from the crater in four mutually perpendicular directions, and then returned (Fig. 15a). The magnetic experiments were conducted at several craters, for example, at the beginning of 2nd and 3rd lunar days (Fig. 15a) and also on the 4th day near Fossa Recta (Fig. 15b and c). This procedure allowed the scientists to measure magnetic parameters of crater slopes, rim, and ejecta, and improved the accuracy of measurements. The experiments revealed that the Moon has a weak magnetic field, but local variations in the direction and intensity of the magnetic field are significant (Ivanov et al., 1977). These results are used to compare the measurements obtained by portable magnetometer during the Apollo missions (Vanyan et al., 1979).

Implementing the traverses for the magnetometer measurements was a complex navigation task. Thus, while performing the experiment on the second lunar day, the Lunokhod-2 traveled

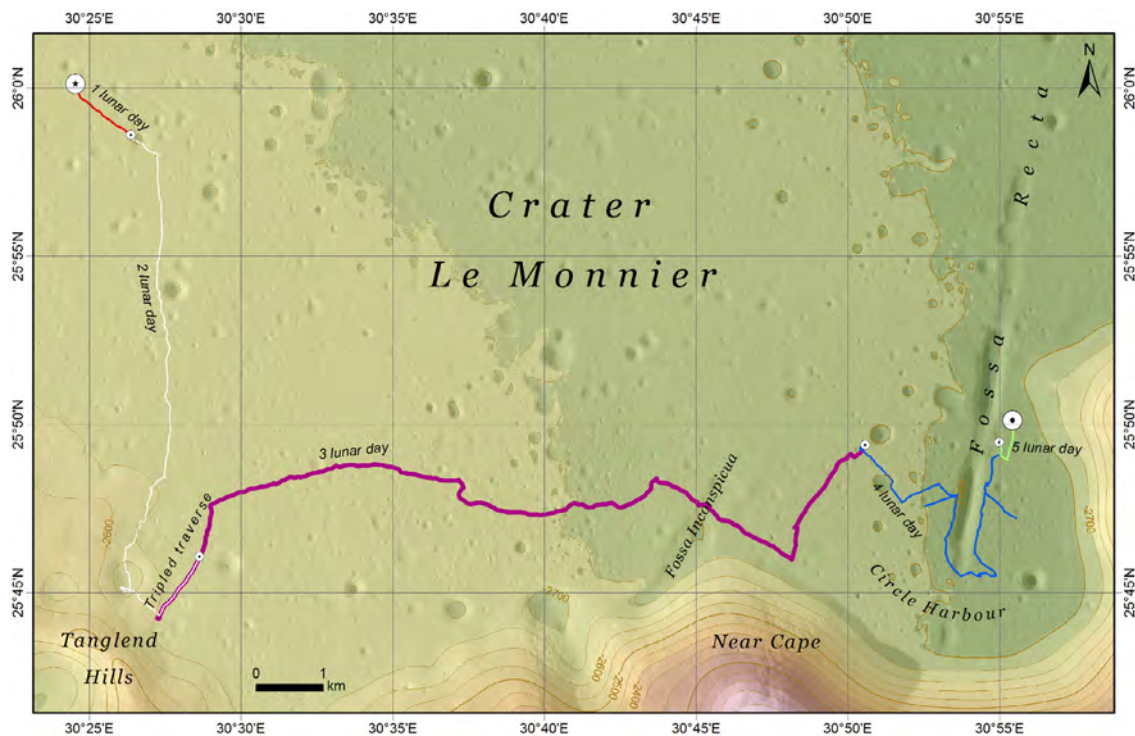


Fig. 18. Hypsometric map of the Lunokhod-2 study area, based on new DEM and orthomosaic.

364 m and made 120 different maneuvers, working 11 h around a crater having a 15-m diameter (Dovgan, 2015). The complexity of navigating around a similar sized crater is shown in Fig. 16a using MKTV-images, that have much lower quality than the panoramas (Fig. 16b).

After completion of the magnetic experiments on the third lunar day, the rover returned to the mare and moved eastward toward the Fossa Recta graben. Lunokhod-2 produced two distance records on this day, covering 17.6 km during 10 sessions (16.6 km according to measurements at the time of the mission) as well as covering 3130 m in one session (Dovgan, 2015). In contrast, the entire Lunokhod-1 traverse during 11 lunar days was 9.9 km as derived from recent GIS-measurements (Karachevtseva et al., 2013), which also differ from the measurements at the time of the mission by  $\sim 0.5$  km.

The rover stopped for the third night about 1.5 km from the graben Fossa Recta ( $\sim 19$  km length,  $\sim 400$  m width,  $\sim 20$  to 50 m depth). During the fourth lunar day, on reaching Fossa Recta, Lunokhod-2 took several panoramas and made measurements of the magnetic field (Fig. 15b). During this day the rover succeeded in traversing around the southern edge of the graben and traveling northward along its eastern rim. The magnetic field was measured in symmetric locations on the western and eastern side, providing a nearly full magnetic profile of the area surrounding Fossa Recta (Fig. 15c).

During four lunar days Lunokhod-2 traversed a total of 38.1 km. The fifth lunar day was the last of the Lunokhod-2 journey and covered a distance of  $\sim 1$  km. The final signal from Lunokhod-2 came on May 10, 1973. Lunokhod-2 parked facing southeast with the lid still open (see Fig. 17). Rover tracks approach from the north to the final parking place. The inset of Fig. 17 is a zoomed-in view of the rover.

## 5. Conclusions

We report on Lunokhod-2 traverse measurements based on photogrammetrically processed NAC images that were used to map

the study region (Fig. 18). Using GIS tools we reconstructed the rover traverse and derived improved locations for points of interest (Table 7) that provide new insights into mission achievements. Lunokhod-2 traversed a total distance of 39.1 km (in contrast to the previous estimate of 37 km); the traverse was four times longer than that of Lunokhod-1.

The main goals of the Lunokhod-2 mission were to investigate the morphology of the transition zone between lunar mare and highland terrains based on the surface panoramic images (Fig. 19a and b). Magnetometer measurements showed variations in the surface magnetic field, suggesting the induction of currents in the Moon under the influence of the changing interplanetary field. Based on laser ranging measurements to the reflector of Lunokhod-2, the rover's final position is one of the best known positions on the Moon, which is used for establishment of the lunar coordinate frame (Archinal et al., 2011) and for studies in lunar orbital and rotational dynamics (Kopeikin et al., 2008).

The DEM, the orthomosaic, and the digitized rover route were used to determine the Lunokhod-2 panorama observation points and for georeferencing of the panoramas in the frame of the ProViDE project (<http://www.provide-space.eu/>), which focused on assembling a major portion of the imaging data gathered so far from vehicles and probes on planetary surfaces into a unique geodatabase.

Bringing archive data into modern spatial context provides excellent opportunities for detailed comparative analysis with new data. It provides a new view on past and recent lunar missions as, for example, studies of Lunokhod-1 and Yutu working areas (Basilevsky et al., 2015), including morphometric and geologic assessment, estimations of boulder types and densities, crater classes, and regolith structure. Moreover, the well-studied lunar regions can be used for future missions as an analog for testing and calibration of different instruments and techniques. For example, high-resolution DEMs and orthomosaics of the Lunokhod-1 and 2 areas support morphometric and safety assessments for selection of candidate Luna-25 (Luna-Glob) landing sites. There is a considerable amount of shadow in polar areas and there is no op-

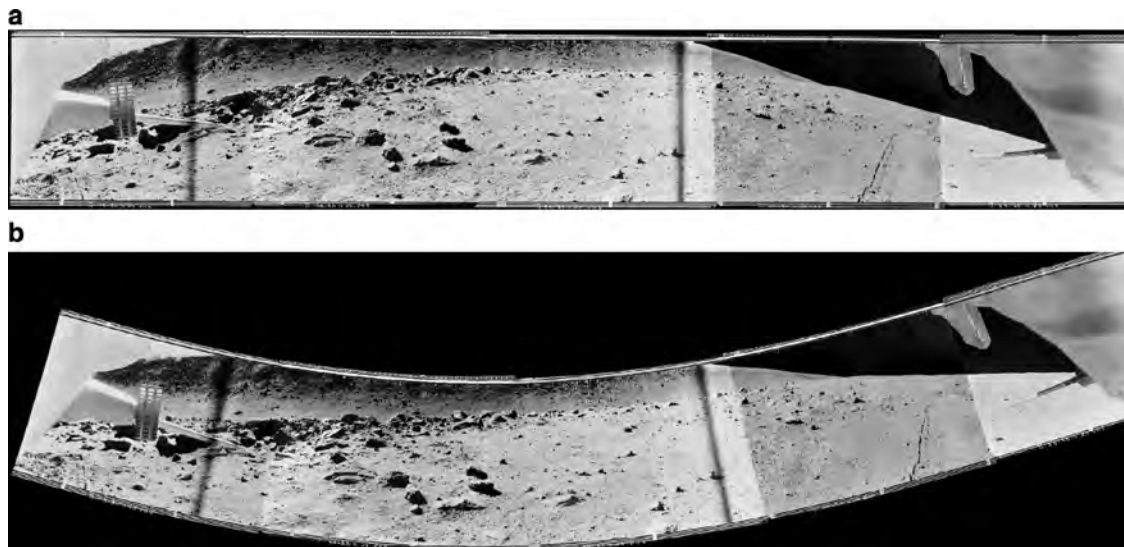


**Fig. 19.** Example one of the last Lunokhod-2 images (#6-448), taken near Fossa Recta: (a) archive panorama in spherical projection; and (b) the same panorama image, which was photogrammetrically transformed to the horizon.

portunity to obtain good quality stereo pairs for photogrammetrically processed DEMs. Therefore, a method of estimating the distribution of slopes in portions of shaded areas measured in the images acquired at different solar incidence angles was suggested (Abdrakhimov et al., 2015). This method was calibrated on analog regions in Lunokhod-1 and 2 areas where we have images with various illumination conditions as well as detailed DEMs. Furthermore, the LLR coordinates of the Lunokhod-1 and 2 rover positions provide high absolute accuracy of the created DEMs that can be used as a reference area to control calibration of the stereo camera for planned Russian Moon projects and to perform refinement of the spacecraft trajectory during the future orbital mission Luna-26 (Luna-Resource).

All digital data products shown in this paper derived from LROC NAC processing as well as newly processed lunar archive panoramas georeferenced to Lunokhod traverse can be found at MIIGAIK Planetary Data Geoportal (<http://cartsrv.mexlab.ru/geoportal/>).

#### Web references

<http://cartsrv.mexlab.ru/geoportal/>  
<http://naif.jpl.nasa.gov/naif/data.html>  
<http://wms.lroc.asu.edu/lroc>  
<http://www.esri.com/>  
<http://www.laspacespace.ru/rus/luna21.html>  
<http://www.laspacespace.ru/rus/museum.php>  
<http://www.provide-space.eu/>  
<http://www.racurs.ru/?page=634>  
<https://isis.astrogeology.usgs.gov/>

#### Acknowledgments

The authors greatly acknowledge useful discussions with G.A. Burba. Also, we wish to thank V.G. Dovgan, member of Lunokhods crew, one of the two drivers who operated the rover remotely, and provided accounts and insights on the Lunokhod missions. We acknowledge and appreciate the work of Ryan Clegg-Watkins and Michael Zanetti at Washington University in St. Louis to trace the Lunokhod-2 tracks in NAC images and for their help in determining the correct traverse distance. Bob Craddock (Smithsonian Institution) and an anonymous reviewer provided valuable comments, which improved an earlier version of this manuscript.

I.P. Karachevtseva, N.A. Kozlova, A.A. Kokhanov, A.E. Zubarev, I.E. Nadezhkina, V.D. Patratiy, A.A. Konopikhin, A.T. Basilevsky and J. Oberst are supported by the Russian Science Foundation (Project no. 14-22-00197).

The processing of archive lunar panoramas received funding from the European Community's Seventh Framework Programme (FP7/2007-2013) under Grant agreement no. 312377 ProViDE.

We wish to thank the Russian State Archive for access and permission to use the scanned raw images.

#### Supplementary materials

Supplementary material associated with this article can be found, in the online version, at [doi:10.1016/j.icarus.2016.05.021](https://doi.org/10.1016/j.icarus.2016.05.021).

#### References

- Abdrakhimov, A.M., Basilevsky, A.T., Head, J.W., et al., 2011. Luna 17/Lunokhod 1 and Luna 21/Lunokhod 2 landing sites as seen by the Lunokhod and LRO cameras. In: Proceedings of the 42nd Lunar and Planetary Science Conference, Abstract #1608, p. 2220.
- Abdrakhimov, A.M., Basilevsky, A.T., Ivanov, M.A., et al., 2015. Occurrence probability of slopes on the lunar surface: Estimate by the shaded area percentage in the LROC NAC images. *Sol. Syst. Res.* 49 (5), 285–294. doi:10.1134/S0038094615050019.
- Abdrakhimov, A.M., 2009. Re-examine Lunokhod Sites: Old and new geochemical data. In: Proceedings of the 40th Lunar and Planetary Science Conference, Abstract #2547.
- Adrov, V.N., Chekurin, A.D., Sechin, A.Yu., et al., 1995. Program PHOTOMOD: digital photogrammetry and stereoscopic image synthesis on a personal computer. In: Fedosov, E.A. (Ed.), Proceedings of SPIE, 2646, Digital Photogrammetry and Remote Sensing'95, pp. 89–96. doi:10.1117/12.227853.
- Anderson, J.A., Sides, S.C., Soltész, D.L., et al., 2004. Modernization of the integrated software for imagers and spectrometers. In: Proceedings of the 35th Lunar and Planetary Science Conference, Abstract #2039.
- Anisov, K.S., Mastakov, V.I., Ivanov, O.G., et al., 1971. General design and assembling of Luna 17 spacecraft. In: Vinogradov, A.P. (Ed.), Mobile Laboratory on the Moon Lunokhod-1, vol. 1. Nauka, pp. 7–20 (in Russian).
- Archinal, B.A., A'Hearn, M.F., Bowell, E., et al., 2011. Report of the IAU working group on cartographic coordinates and rotational elements: 2009. *Celest. Mech. Dyn. Astron.* 109 (2), 101–135.
- Barsukov V.L. (Ed.). Mobile Laboratory on the Moon Lunokhod-1, vol. 2. Nauka Moscow. 1978, p. 183. (in Russian).
- Basilevsky, A.T., Kreslavsky, M.A., Karachevtseva, I.P., et al., 2014. Morphometry of small impact craters in the Lunokhod-1 and Lunokhod-2 study areas. *Planet. Space Sci.* 92, 77–87.
- Basilevsky, A.T., 1976. On the evolution rate of small lunar craters. In: Proceedings of the 7th Lunar and Planetary Science Conference, pp. 1005–1020.
- Basilevsky, A.T., Abdrakhimov, A.M., Head, J.W., et al., 2015. Geologic characteristics of the Luna 17/Lunokhod 1 and Chang'E-3/Yutu landing sites, Northwest Mare

- Imbrium of the Moon. *Planet. Space Sci.* 117, 385–400. doi:10.1016/j.pss.2015.08.006.
- Basilevsky, A.T., Abdrakhimov, A.M., Ivanov, M.A., et al., 2012. Identification and measurements of small impact craters in the Lunokhod 1 study area, Mare Imbrium. In: *Proceedings of the 43rd Lunar and Planetary Science Conference*, Abstract #1481.
- Becker, K.J., Archinal, B.A., Hare, T.M., et al., 2015. Criteria for automated identification of stereo image pairs. In: *Proceedings of the 46th Lunar and Planetary Science Conference*, Abstract #2703.
- Beigman, I.L., Vainshtein, L.A., Vasiliev, B.N., et al., 1978. X-ray collimator telescope RT-1. In: Barsukov, A.P. (Ed.), *Mobile Laboratory on the Moon Lunokhod-1*, vol. 2. Nauka, Moscow, pp. 136–141 (in Russian).
- Cherkašov, I.I., Shvarev, V.V., 1975. *Lunar Ground*. Nauka, Moscow, p. 142 (in Russian).
- Clegg, R.N., Jolliff, B.L., Robinson, M.S., et al., 2014. Effects of rocket exhaust on lunar soil reflectance properties. *Icarus* 227, 176–194. doi:10.1016/j.icarus.2013.09.013.
- Dickey, J.O., Bender, P.L., Faller, J.E., et al., 1994. Lunar laser ranging: a continuing legacy of the Apollo program. *Science* 265, 482–490.
- Dolginov, Sh., Yeroshenko, Ye.G., Shapova, V.A., et al., 1976. Study of magnetic field, rock magnetization and lunar electrical conductivity in the Bay Le Monnier. *Moon* 15, 3–14.
- Dovgan, V.G., 2015. The Moon Odysseus of Soviet Cosmonautics'. From "Mechta" ("Dream") to the Moon Rovers. *Southern Federal University*, Rostov-on-Don, p. 307 (in Russian).
- Elenov, A.I., Rybin, A.M., Yakovlev, A.S., 1971. Thermal conditions and temperature control system. In: Vinogradov, A.P. (Ed.), *Mobile Laboratory on the Moon Lunokhod-1*, vol. 1. Nauka, Moscow, pp. 30–33 (in Russian).
- Florensky, K.P., Basilevsky, A.T., Bobina, N.N., et al., 1976. Processes of the transformation of the lunar surface in the Le Monnier region studied using results of detailed investigations made by Lunokhod 2. In: *Tectonics and Structural Geology. Planetology; International Geological Congress, Session, 25th. Sydney, Australia, August 16–25, 1976*, pp. 205–234. Reports. (A78-16366 04-91). Moscow, Nauka, 1976 (in Russian).
- Florensky, K.P., Bazilevsky, A.T., Gurshteyn, A.A., et al., 1974. Geological and morphological analysis of the "Lunokhod-2" work area. *Rep. USSR Acad. Sci.* 214 (1), 75–78 (in Russian).
- Florensky, K.P., Bazilevsky, A.T., Zezin, R.B., et al., 1978. Geologic and morphologic study of lunar surface. In: Barsukov, A.P. (Ed.), *Mobile Laboratory on the Moon Lunokhod-1*, Vol. 2. Nauka, Moscow, pp. 102–135 (in Russian).
- Grodecki, J., Dial, G., 2003. Block adjustment of high-resolution satellite images described by rational polynomials. *Photogram. Eng. Remote Sens.* 69 (1), 59–68.
- Haase, I., Oberst, J., Scholten, F., Wählisch, M., et al., 2011. Mapping the Apollo 17 landing site area based on Lunar Reconnaissance Orbiter Camera images and Apollo surface photography. *J. Geophys. Res.* 117, 1–8. E00H20.
- Hirschmüller, H., 2005. Accurate and efficient stereo processing by semi-global matching and mutual information. *Comput. Vis. Pattern Recognit.* 2, 807–814.
- Huntress, W.T., Marov, M.Y., 2011. *Soviet Robots in the Solar System*. Springer Praxis Books, p. 453.
- Ivanov, B.A., Okulesky, B.A., Bazilevsky, A.T., 1977. Shock wave, a possible source of magnetic fields? In: Roddy, D.J., Pepin, R.O., Merrill, R.H. (Eds.), *Impact and Explosion Cratering*. Pergamon Press, New York, pp. 861–867.
- Karachevtseva, I., Oberst, J., Scholten, F., et al., 2013. Cartography of the Lunokhod-1 landing site and traverse from LRO image and stereo topographic data. *Planet. Space Sci.* 85, 175–187. <http://dx.doi.org/10.1016/j.pss.2013.06.002>.
- Keller, J.W., Petro, N.E., Vondrak, R.R., 2016. The Lunar Reconnaissance Orbiter Mission - Six years of science and exploration at the Moon. *Icarus* 273, 2–24. doi:10.1016/j.icarus.2015.11.024.
- Kemurdzhian A.L. (Ed.), 1993. *The Rovers*. Mashinostroenie, Moscow. 400 p. (in Russian).
- Kemurdzhian, A.L., Gromov, V.V., Shvarev, V.V., 1978. Investigation of physical and mechanical properties of extraterrestrial soil. In: Vernov, S.N. (Ed.), *Soviet Achievements in Space Exploration 1967–1977*. Nauka, Moscow, pp. 352–380 (in Russian).
- Kocharov, G.E., Borodulin, N.F., Viktorov, S.V., et al., 1971. Lunar automatic spectrometric equipment RIFMA (RHYME). In: Vinogradov, A.P. (Ed.), *Mobile Laboratory on the Moon Lunokhod-1*, vol. 1. Nauka, Moscow, pp. 89–95 (in Russian).
- Kocharov, G.E., Viktorov, S.V., 1974. The chemical composition of the lunar surface in the work region of the Lunokhod-2. *Rep. USSR Acad. Sci.* 214 (1), 71–74 (in Russian).
- Kokurin, Yu.L., 2003. Lunar laser ranging. 40 years of research. *Quantum Electron.* 33 (1), 45–47 (in Russian).
- Kokurin, Yu.L., Kurbasov, V.V., Lobanov, V.F., et al., 1978. Laser radar location experiment using light reflector mounted on the Lunokhod-1 vehicle. In: Barsukov, V.L. (Ed.), *Mobile Laboratory on the Moon Lunokhod-1*, vol. 2. Nauka, Moscow, pp. 170–180 (in Russian).
- Kopeikin, S., Pavlis, E., Pavlis, D., et al., 2008. Prospects in the orbital and rotational dynamics of the Moon with the advent of sub-centimeter lunar laser ranging. *Adv. Space Res.* 42 (8), 1378–1390. doi:10.1016/j.asr.2008.02.014.
- Kozlova N., Zubarev A., Karachevtseva I., et al. Some aspects of modern photogrammetric image processing of Soviet Lunokhod panoramas and their implementation for new studies of lunar surface. In: *The International Archives of the Photogrammetry, Remote Sensing and Spatial Information Sciences. ISPRS Technical Commission IV Symposium*, Suzhou, China, 2014, vol. XL-4, pp. 121–126. doi:10.5194/isprsarchives-XL-4-121-2014.
- Leonovich, A.K., Ivanov, O.G., Pavlov, P.S., et al., 1978. Self-propelled chassis Lunokhod-1 as a tool for the study of lunar surface. In: Barsukov, A.P. (Ed.), *Mobile Laboratory on the Moon Lunokhod-1*, vol. 2. Nauka, Moscow, pp. 25–43 (in Russian).
- Leonovich, A.K., Gromov, V.V., Rybakov, A.V., et al., 1971. Studies of the mechanical properties of lunar soil on self-propelled vehicle Lunokhod-1. In: Vinogradov, A.P. (Ed.), *Mobile Laboratory on the Moon Lunokhod-1*, vol. 1. Nauka, Moscow, pp. 78–88 (in Russian).
- Lipskiy, Yu.N., Rodionova, Zh.F., 1978. Cartography of the Moon. In: Vernov, S.N. (Ed.), *Soviet Achievements in Space Exploration 1967–1977*. Nauka, Moscow, pp. 406–434 (in Russian).
- Mazarico, E., Rowlands, D.D., Neumann, G.A., et al., 2012. Orbit determination of the Lunar Reconnaissance Orbiter. *J. Geod.* 86 (3), 193–207. doi:10.1007/s00190-011-0509-4.
- Murphy Jr, T.W., Adelberger, E.G., Battat, J.B.R., et al., 2010. Long-term degradation of optical devices on the Moon. *Icarus* 208, 31–35.
- Murphy, T.W., Adelberger, E.G., Battat, J.B.R., et al., 2011. Laser ranging to the lost Lunokhod 1 reflector. *Icarus* 211 (2), 1103–1108.
- Oberst, J., Scholten, F., Matz, K.D., et al., 2010. Apollo 17 landing site topography from LROC NAC stereo data – First analysis and results. In: *Proceedings of the 41st Lunar and Planetary Science Conference*, Abstract #2051. Houston TX.
- Petrov, Yu.A., 1978. Psychological problems of remote control. In: Barsukov, A.P. (Ed.), *Mobile Laboratory on the Moon Lunokhod-1*, vol. 2. Nauka, Moscow, pp. 20–25 (in Russian).
- Researches of the Moon, Chapter 4, pp. 142–214. In: *Development of a space in the USSR, 1973* (On Press Materials). Nauka, Moscow. 1975. 305 p. (in Russian).
- Robinson, M.S., Brylow, S.M., Tschimmel, M., et al., 2010. The Lunar Reconnaissance Orbiter Camera (LROC) instrument overview. *Space Sci. Rev.* 150, 81–124.
- Rodionov, B.N., 1999. To the history of the lunar exploration by Soviet spacecraft. In: *Proceedings of the International Symposium "The Scientific Results of Space Research of the Moon. 40th Anniversary of the First Images of Far Side of the Moon"*. Sternberg State Astronomical Institute, Moscow (in Russian).
- Rodionov, B.N., Nepoklonov, B.V., Kiselev, V.V., 1971. Topography study along the "Lunokhod-1" route. In: Vinogradov, A.P. (Ed.), *Mobile Laboratory on the Moon Lunokhod-1*, vol. 1. Nauka, Moscow, pp. 55–73 (in Russian).
- Rodionov, B.N., Nepoklonov, B.V., Kiselev, V.V., et al., 1973. Topographical surveys on the lunar surface from the Soviet unmanned spacecrafts. *Geod. Cartogr.* 10, 29–41 (in Russian).
- Scholten, F., Oberst, J., Matz, K.-D., et al., 2012. GLD100: The near-global lunar 100 m raster DTM from LROC WAC stereo image data. *J. Geophys. Res.* 117, 1–12. E00H17.
- Sechin, A., 2014. Dense DSM generation module in PHOTOMOD 6.0. In: *Proceedings of the 14th International Scientific and Technical Conference "From image to map: digital photogrammetric technologies"*. Hainan, China [http://conf.racurs.ru/images/presentations/SECHIN\\_DSM\\_CHINA.pptx](http://conf.racurs.ru/images/presentations/SECHIN_DSM_CHINA.pptx).
- Selivanov, A.S., Govorov, V.M., Zasetkii, V.V., et al., 1971. Construction properties and main parameters of Lunokhod-1 television systems. In: Vinogradov, A.P. (Ed.), *Mobile Laboratory on the Moon Lunokhod-1*, vol. 1. Nauka, Moscow, pp. 55–65 (in Russian).
- Severyn, A.B., Terez, E.I., Zvereva, A.M., 1975. The measurements of sky brightness on Lunokhod-2. *Moon* 14, 123–128.
- Speyerer, E.J., Wagner, R.V., Licht, A., et al. New SPICE to improve the geodetic accuracy of LROC NAC and WAC images. 2014, 45th Lunar and Planetary Science Conference. Abstract #2421.pdf.
- Speyerer, E.J., Wagner, R.V., Robinson, M.S., et al., 2012. In-flight geometric calibration of the lunar reconnaissance orbiter camera. In: *The International Archives of the Photogrammetry, Remote Sensing and Spatial Information Sciences*, pp. 511–516. doi:10.5194/isprsarchives-XXXIX-B4-511-2012.
- Stooke, Ph.J., 2007. *The International Atlas of Lunar Exploration*. Cambridge University Press, p. 440.
- Vanyan, L.L., Vnuchkova, T.A., Egorov, I.V., et al., 1979. Electrical conductivity anomaly beneath Mare Serenitatis detected by Lunokhod 2 and Apollo 16 magnetometers. *Moon Planets* 21, 185–192.
- Vernov, S.N., Lyubimov, G.P., Chuchkov, E.A., et al., 1971. The study of cosmic rays. In: Vinogradov, A.P. (Ed.), *Mobile Laboratory on the Moon Lunokhod-1*, vol. 1. Nauka, Moscow, pp. 116–125.
- Viktorov, S.V., Chesnokov, V.I., 1978. *The Chemistry of a Lunar Soil, Series: Astronautics, Astronomy. Znanie*, Moscow, p. 64 (in Russian).
- Vinogradov A.P. (Ed.) *Mobile Laboratory on the Moon Lunokhod-1*, vol. 1. Nauka, Moscow, 1971. p. 128 (in Russian).
- Vondrak, R., Keller, J., Chin, G., et al., 2010. Lunar Reconnaissance Orbiter (LRO): Observations for lunar exploration and science. *Space Sci. Rev.* 150, 7–22. doi:10.1007/s12124-010-9631-5.
- Wagner, R.V., Robinson, M.S., Speyerer, E.J., et al., 2014. Locations of anthropogenic sites on the Moon. In: *Proceedings of the 45th Lunar and Planetary Science Conference*, Abstract #2259.
- Williams, J.G., Boggs, D.H., Folkner, W.M., 2013. DE430 Lunar Orbit, Physical Librations, and Surface Coordinates. Report No. IOM 335-JW, DB, WF-20130722-016. Jet Propulsion Laboratory.
- Zubarev, A.E., Nadezhkina, I.E., Kozlova, N.A., et al., 2016. Special software for planetary image processing and research. In: *Proceedings of The International Archives of the Photogrammetry, Remote Sensing and Spatial Information Sciences* (in press).